Laser Shaping

- Motivation
  - Coherent & Optimal Control
  - Minimizing Emittance
- Transverse shaping
  - Refractive shaper
  - Spatial Light Modulators & Deformable mirrors
  - Truncated Gaussian
- Temporal Shaping
  - Fourier Transform Shaping
  - Acousto-Optic Programmable Dispersive Filter (AOPDF, ‘Dazzler’)
  - Pulse stacking
  - 3d pulse
- Femtosecond Pancake pulse
- Z-polarized pulse

Motivation

Shaping's original impetus came from Atomic, Molecular and Optical (AMO) Physics, with applications in coherent and optimal control in mind.

• Manipulate quantum state interferences through coherent coupling and/or precise timing of transitions

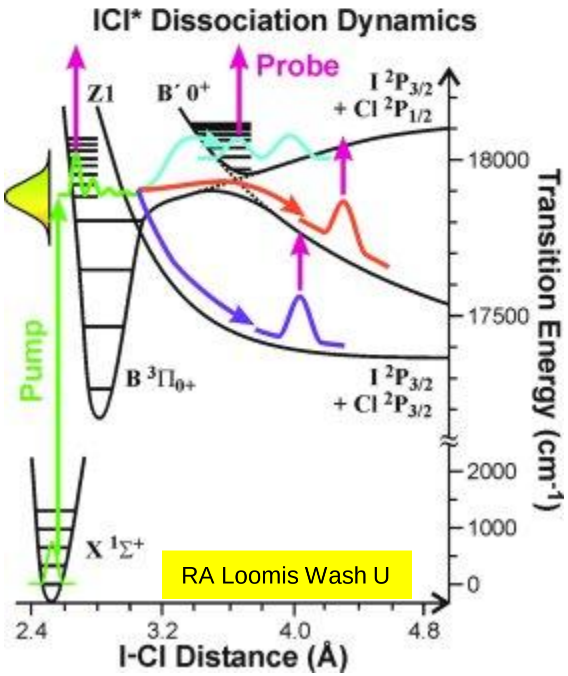

RA Loomis Wash U

controlling branching ratios in photodissociation by coherent manipulation of wavepacket formation

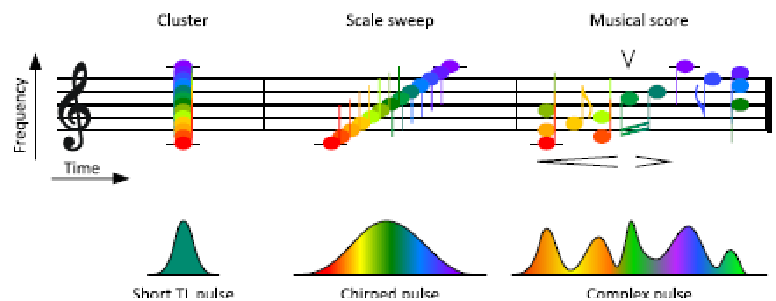

Daan Sprunken
U. Twente

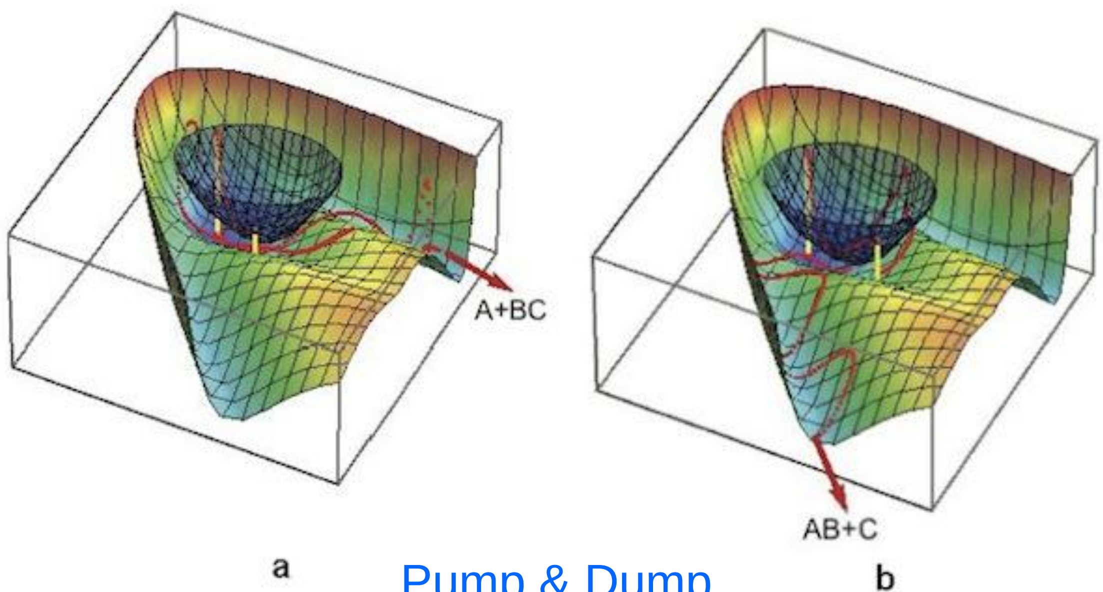

Pump & Dump

S. Varganov U Nev
http://www.chem.unr.edu/faculty/sav/

Shaping at the attosecond level

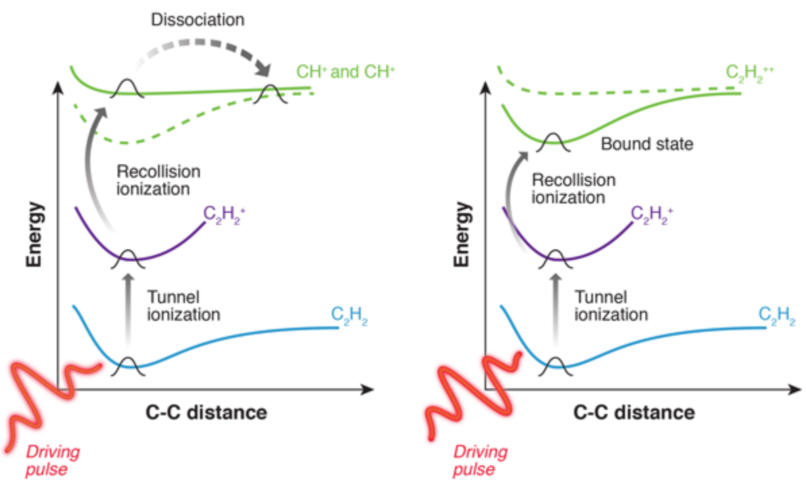

Figure 1: Simplified illustration of the CEP dependent photofragmentation mechanism. (Left) For the CEP value of the driving pulse in the lower left, the kinetic energy of the recolliding electron is high enough to promote the molecule to a dissociative state, leading to photofragmentation. (Right) For this CEP value of the driving pulse, the kinetic energy of the recolliding electron is lower and the molecule is promoted to a bound state, from which photodissociation cannot take place. Carin Cain

Manipulating photofragementation yields through the carrier envelope phase

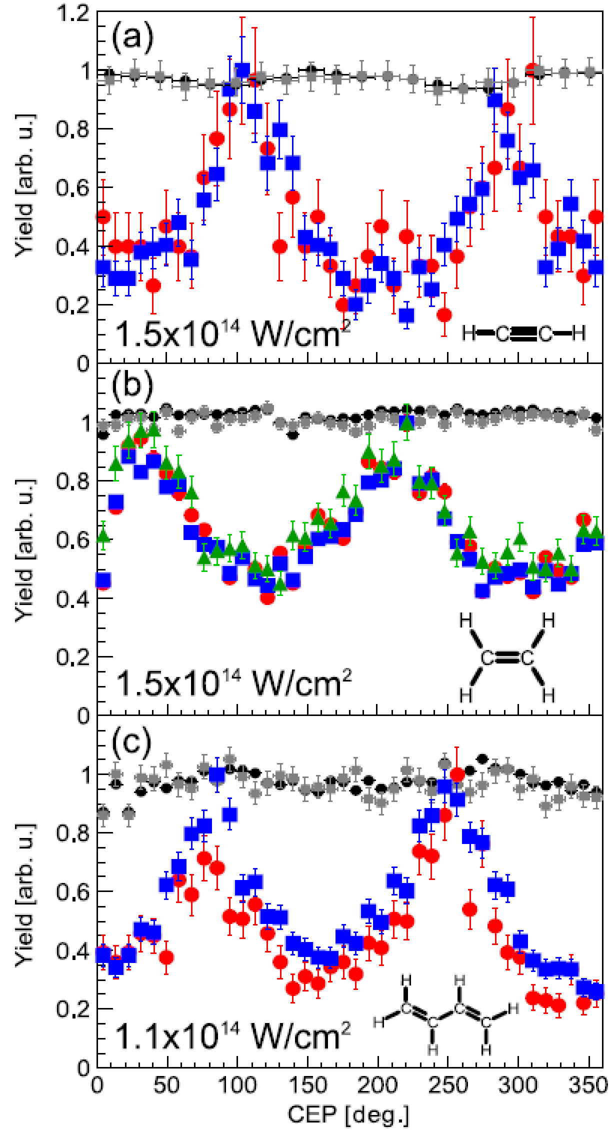

acetylene

ethylene

1,3 butadiene

Carrier Envelope Phase

Xie et al PRL 109, 243001 (2012), and associated Physics Viewpoint

Minimizing emittance

- Space charge forces increase beam emittance
- non-uniform charges create nonlinear space charge forces
- linear forces can be compensated and the emittance minimized

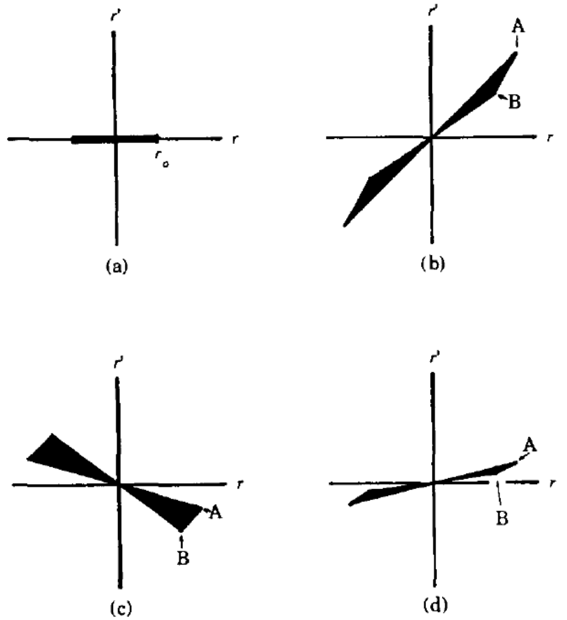

evolution of ‘beer-can’ e-bunch in transverse phase space:
a) at cathode, b) after drift, before lens
c) immediately after lens d) after 2nd drift, after lens

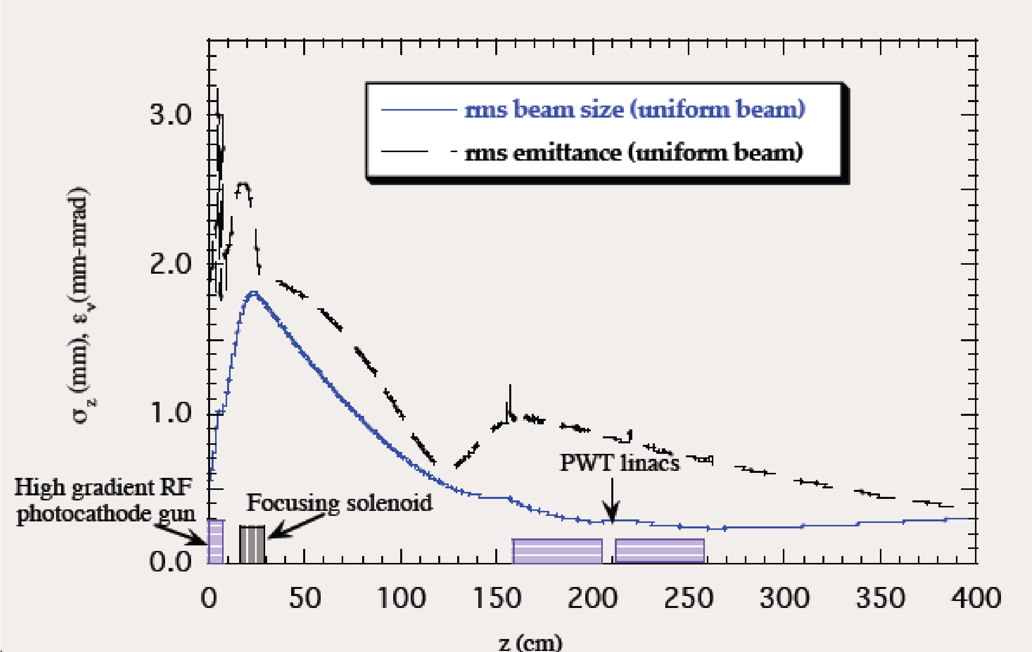

Multiparticle simulations (UCLA PARMELA)
Showing emittance oscillations and minimization

Carlsten, NIMA 285, 313 (1989)

J Rosenzweig JLAB 05

Extra Credit Project

Read the Carlsten NIMA 89 paper referenced on the previous slide and present to the class the analysis behind the figure shown (Fig 3 in the paper).

Minimizing emittance

- Linear space charge forces can be compensated
- Uniform Ellipsoidal (UE) distribution has purely linear SC forces
- ‘Beer can’ or Uniform Cylindrical (UC) a close approximation

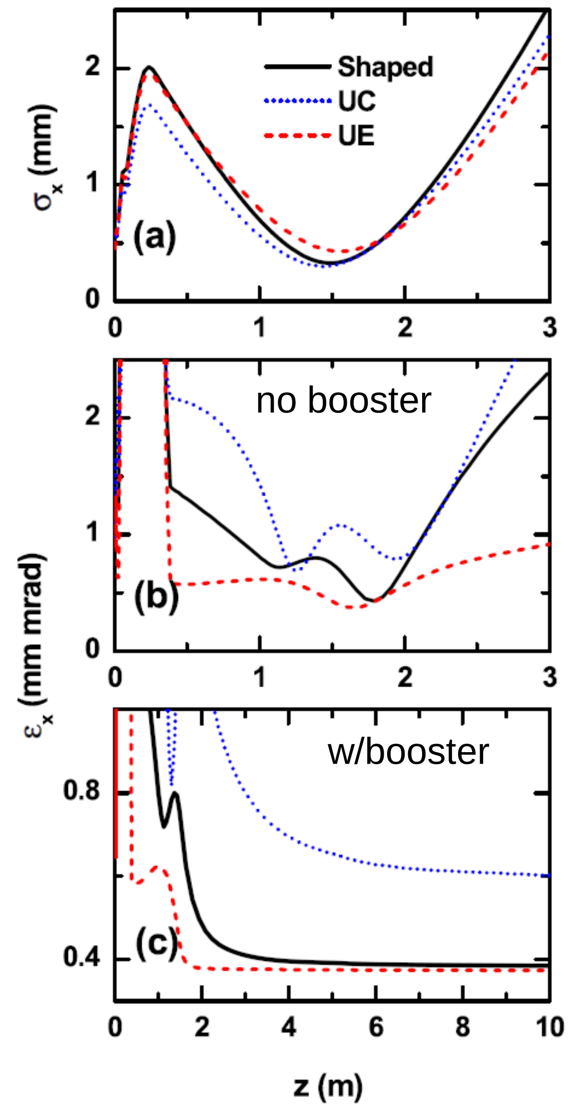

Simulations using LCLS injector conditions →

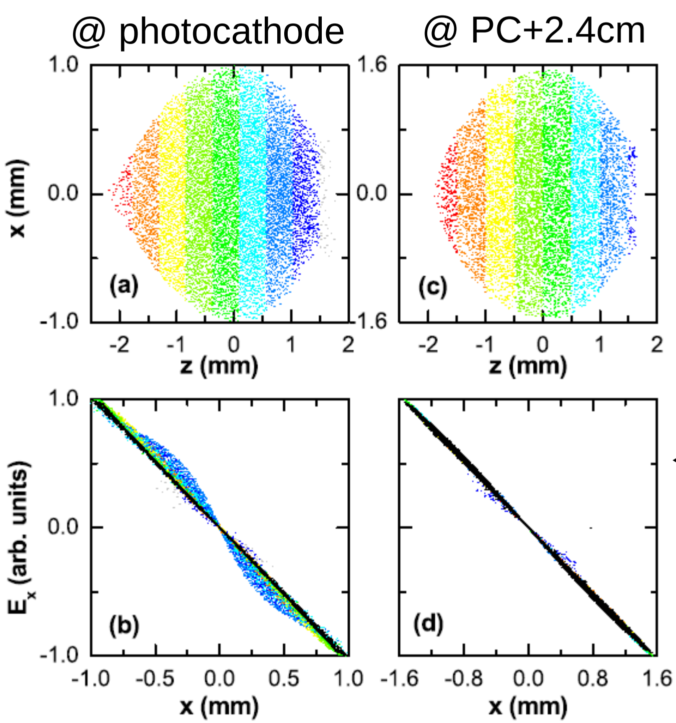

‘Shaped’ =quasi-ellipsoid achieved exploiting chromatic aberration of lens & phase-shaped beam

← color: shaped dist
black: UE dist

Li, Chemerisov & Lewellen, PRSTAB 12, 020702 (2009)

Transverse space charge forces

Gaussian

$$\exp\left[-\frac{1}{2}\left(\frac{r}{R}\right)^2-\frac{1}{2}\left(\frac{t}{T}\right)^2\right]$$

Uniform Cylindrical

Uniform Ellipsoid

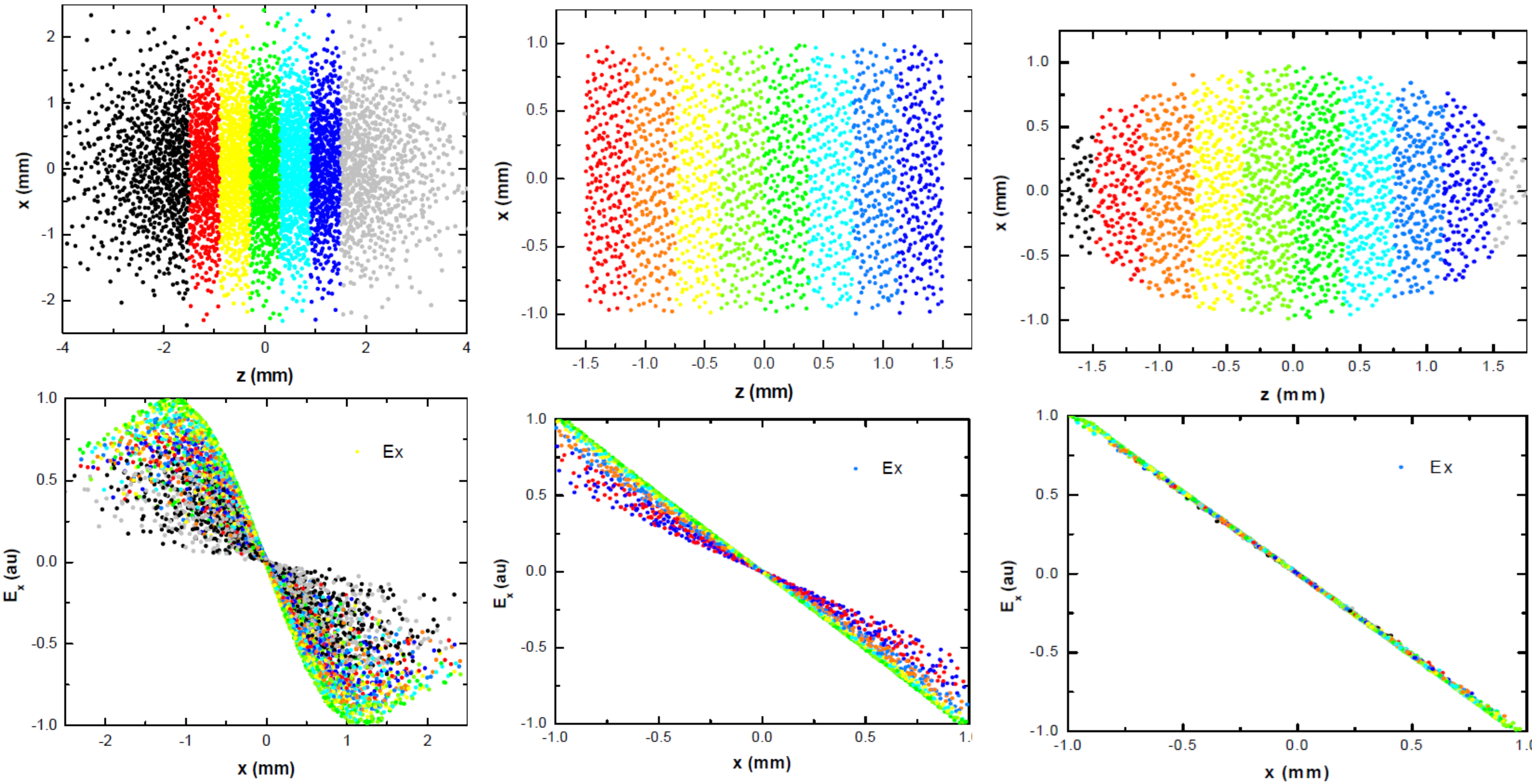

Yuelin Li, USPAS 2008

Longitudinal space charge forces

Gaussian

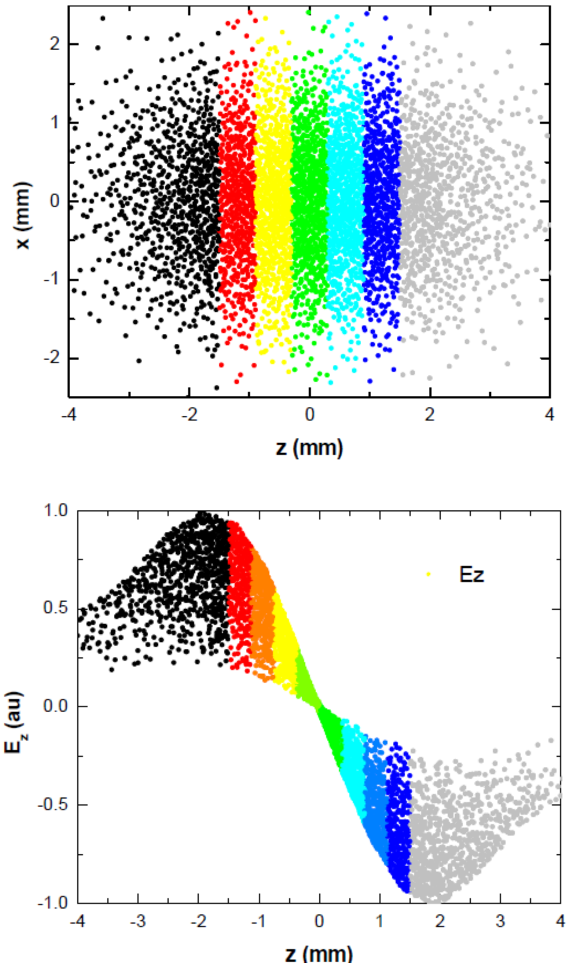

Uniform Cylindrical

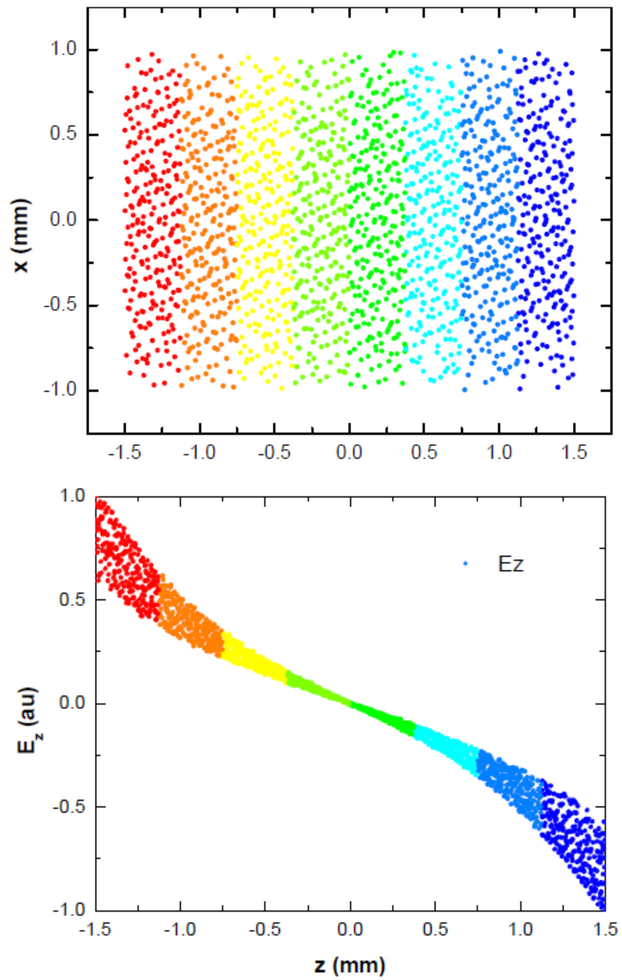

Uniform Ellipsoid

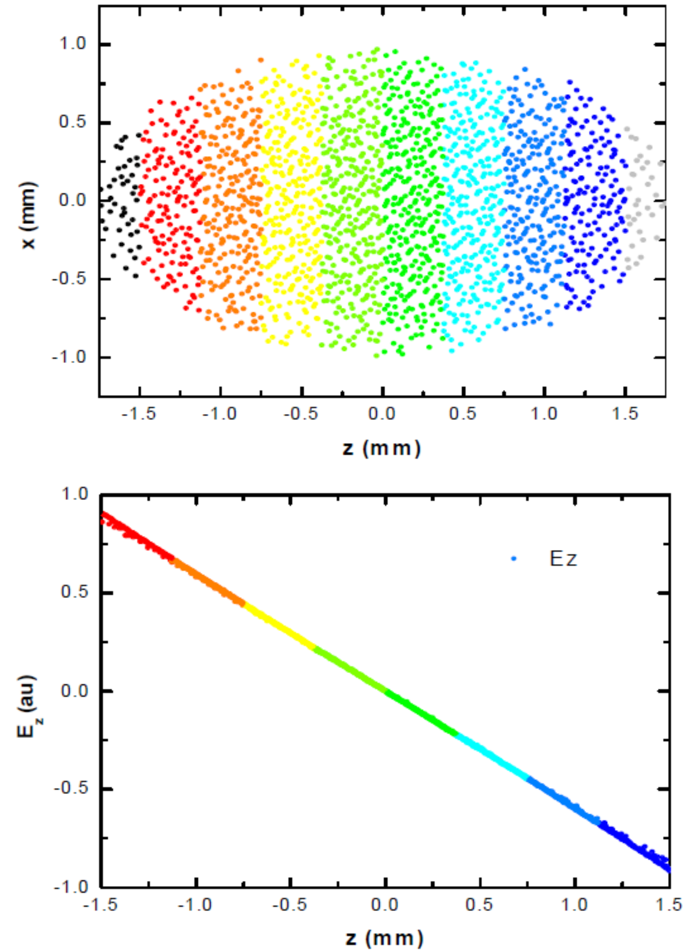

Yuelin Li, USPAS 2008

Transverse Shaping

- Refractive shapers
- Addressable shapers:
  - spatial light modulators
  - deformable mirrors
- Truncated Gaussian

Refractive transverse shaper designs

Newport design

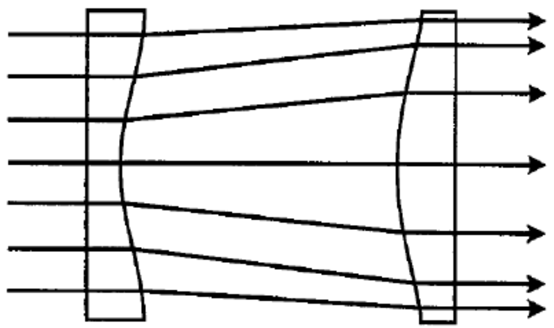

Hoffnagle et al, Apll. Opt. 39 5488 2000).

Singlet design 1

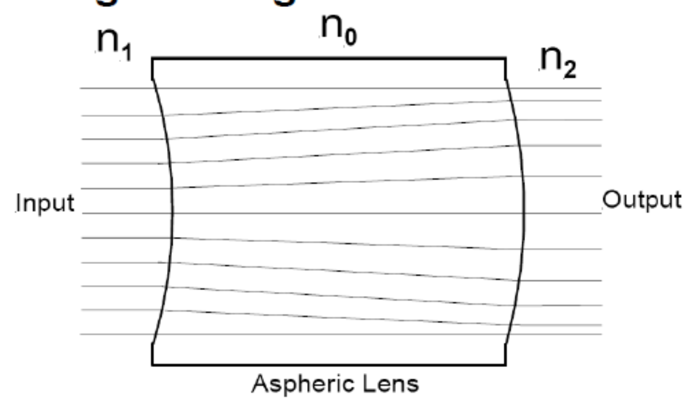

Zhang et al., Opt Express 11, 1942 (2003).

Another 2-lens design

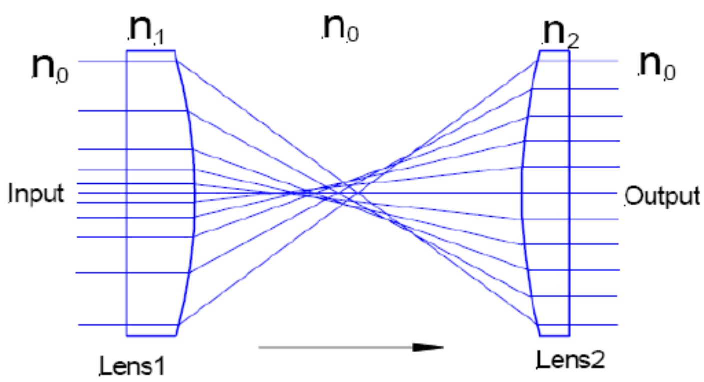

Liu and Zhang et al., Opt. Express 16, 6675 (2008).

Singlet design 2

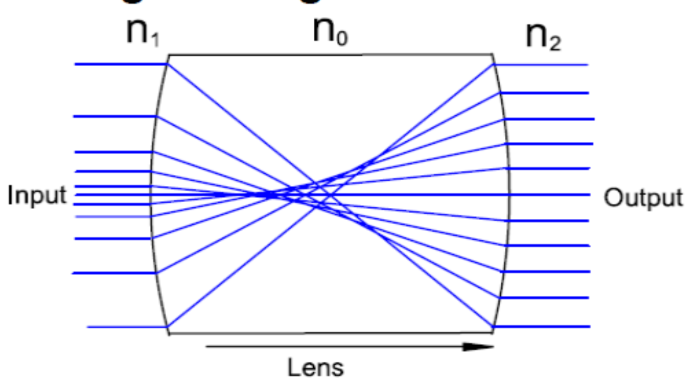

Zhang et al., J. Opt. A9, 945 (2007).

credit: Yuelin Li

Refractive shapers

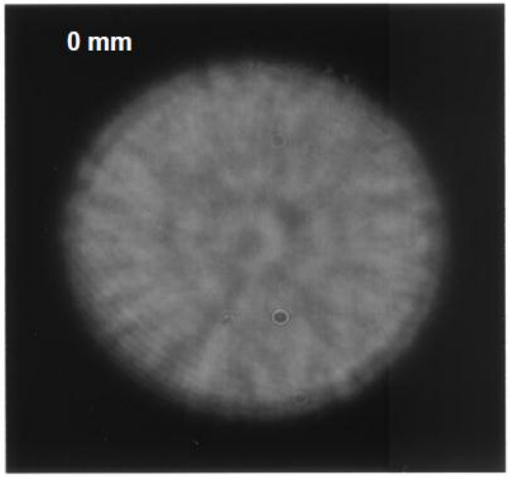

Newport design: intensity distributions as a function of distance from output end.

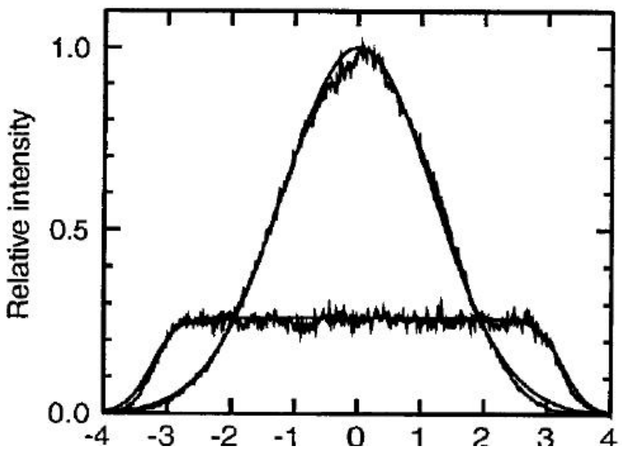

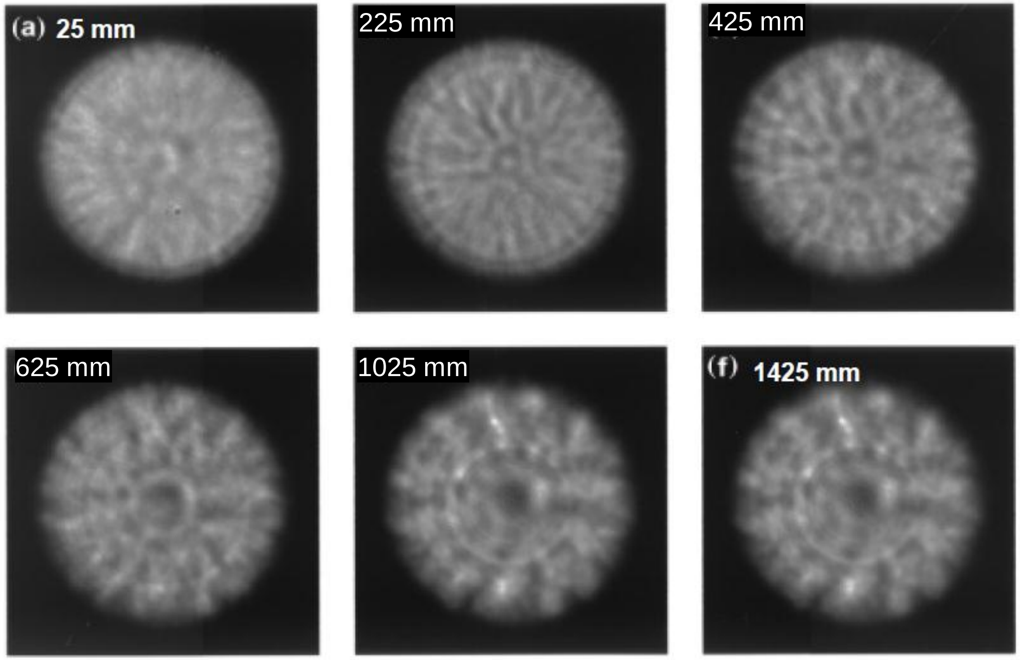

Hoffnagle et al Apl Opt 39, 5488 (2000)

Refractive Shapers

Pros

- simplicity
- efficiency
- multiple designs
- commercially available (Newport, MolTech)

Cons

- sensitivity to input beam shape and alignment
- sensitivity to optics alignment
- depth of field (but can be imaged)

Beam Size ±5% w_0

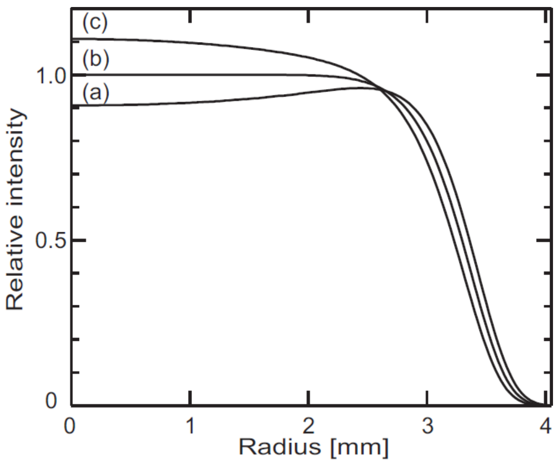

Beam offset 0-10% w_0

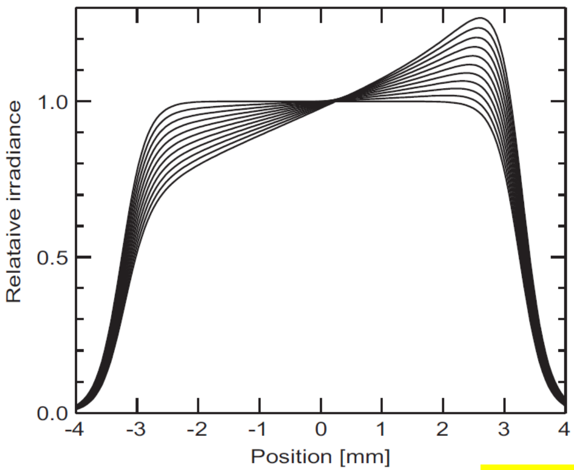

Beam tilt

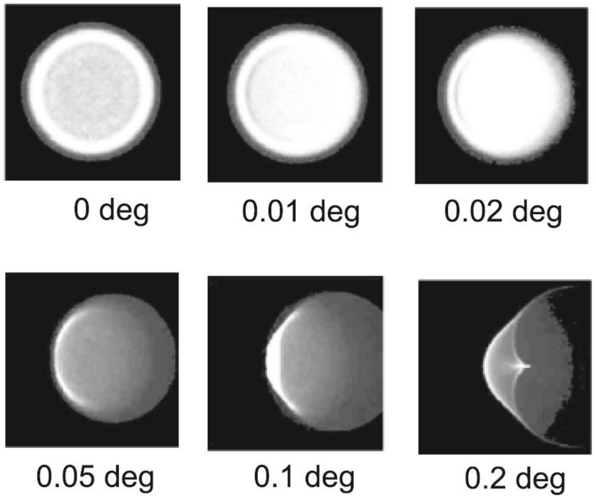

Shealy & Hoffnagle SPIE proc. v 8490 (2012)

Addressable transverse shaping

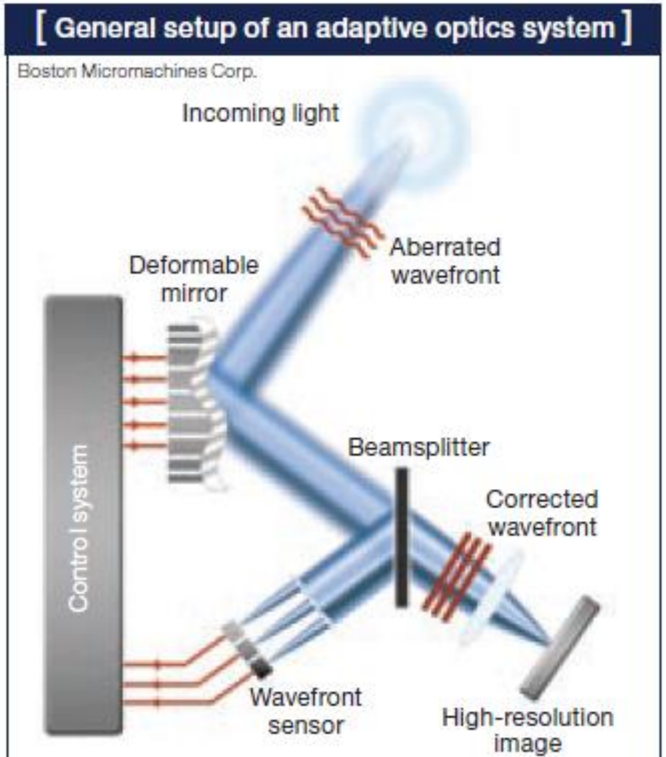

The wavefront sensor (here shown as a Shack-Hartmann sensor) determines the phase errors in the input wavefront. These errors are processed and generate signals to drive a deformable mirror, which corrects the wavefront and provides a higher-resolution image on the detector.

- Wide Range of Applications
- Many different commercially available implementations

10x10 arcsec

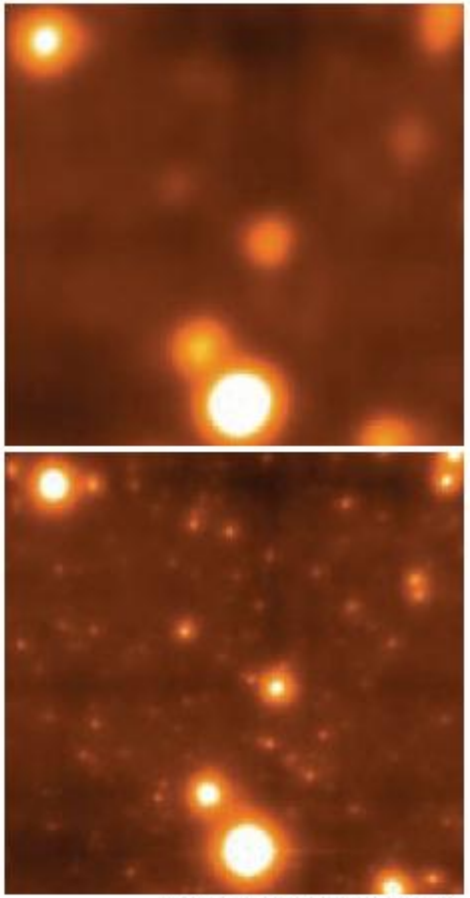

Craig Mackay and Nick Law, Caltech

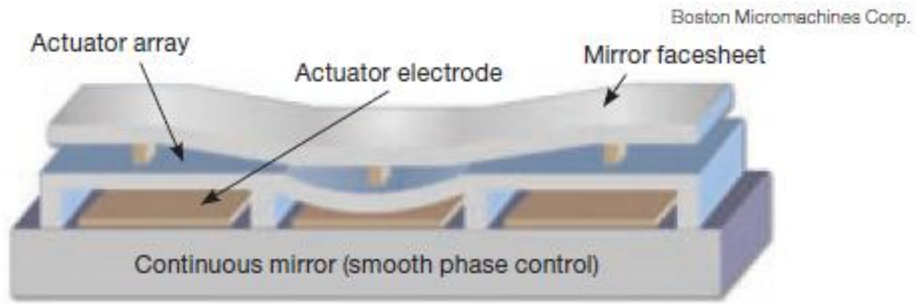

Applying an array of electrical potentials to the electrodes causes the mirror to be deformed. By reflecting the input wavefront with such a device, one can compensate for the phase errors in the incoming wavefront. MEMS deformable mirrors are available with more than 1,000 elements in total.

C MacKay Optics & Photonics News Nov 2009

Spatial Light Modulators(SLM)

Boulder Nonlinear Systems

Nematic SLM

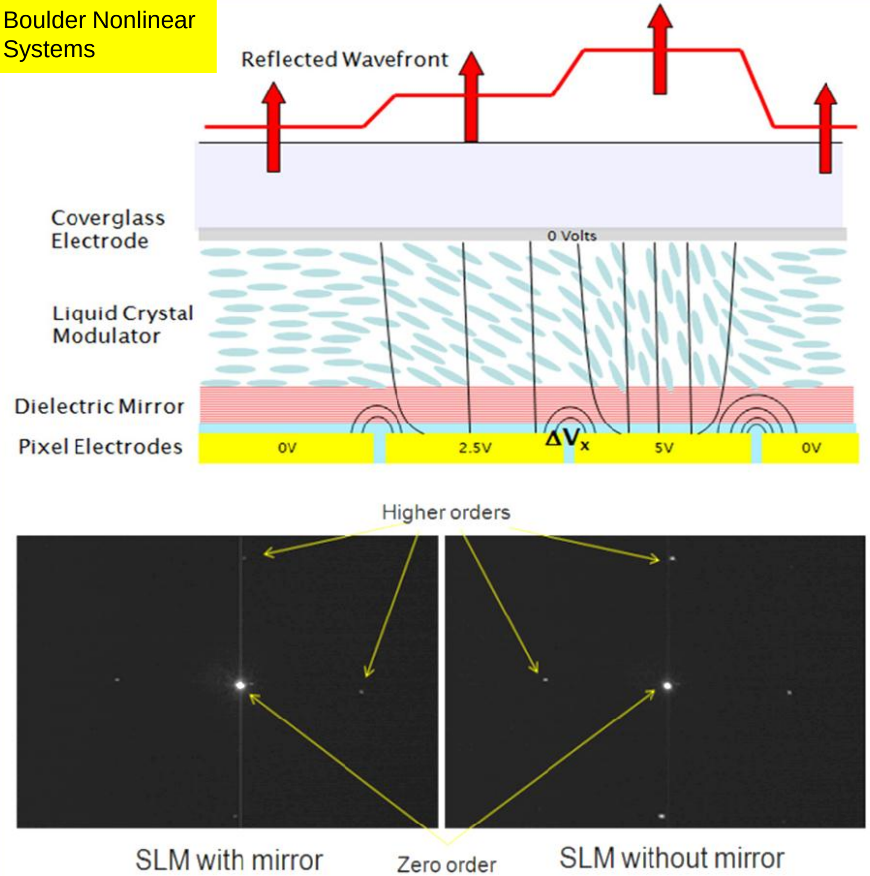

Measured zero-order diffraction efficiency ~ 90%

Measured zero-order diffraction efficiency ~ 61%

DLP* chip element

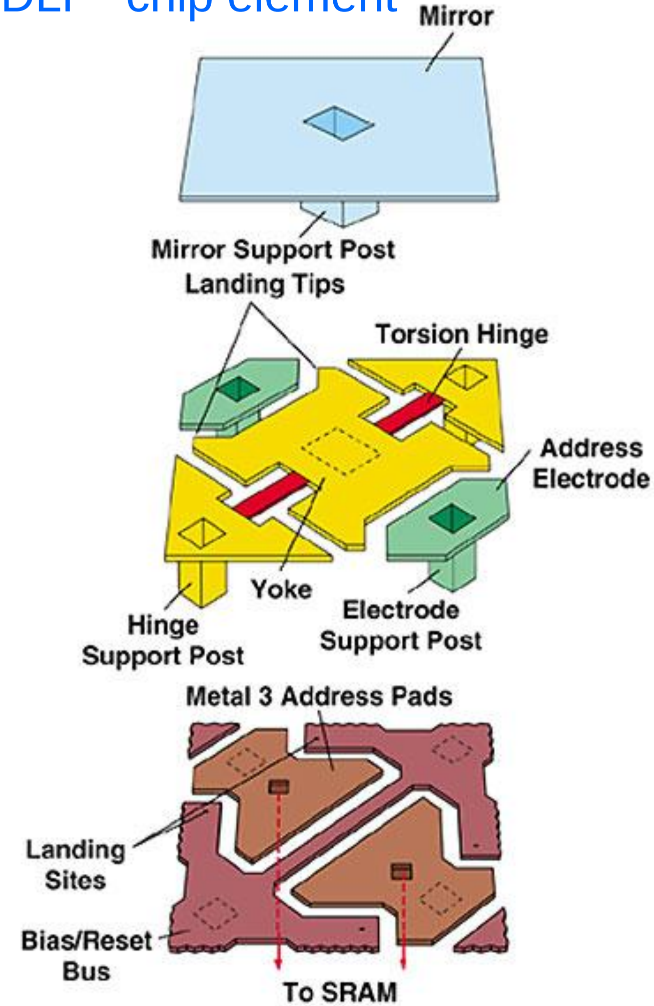

Texas Instruments

*Digital Light Processing

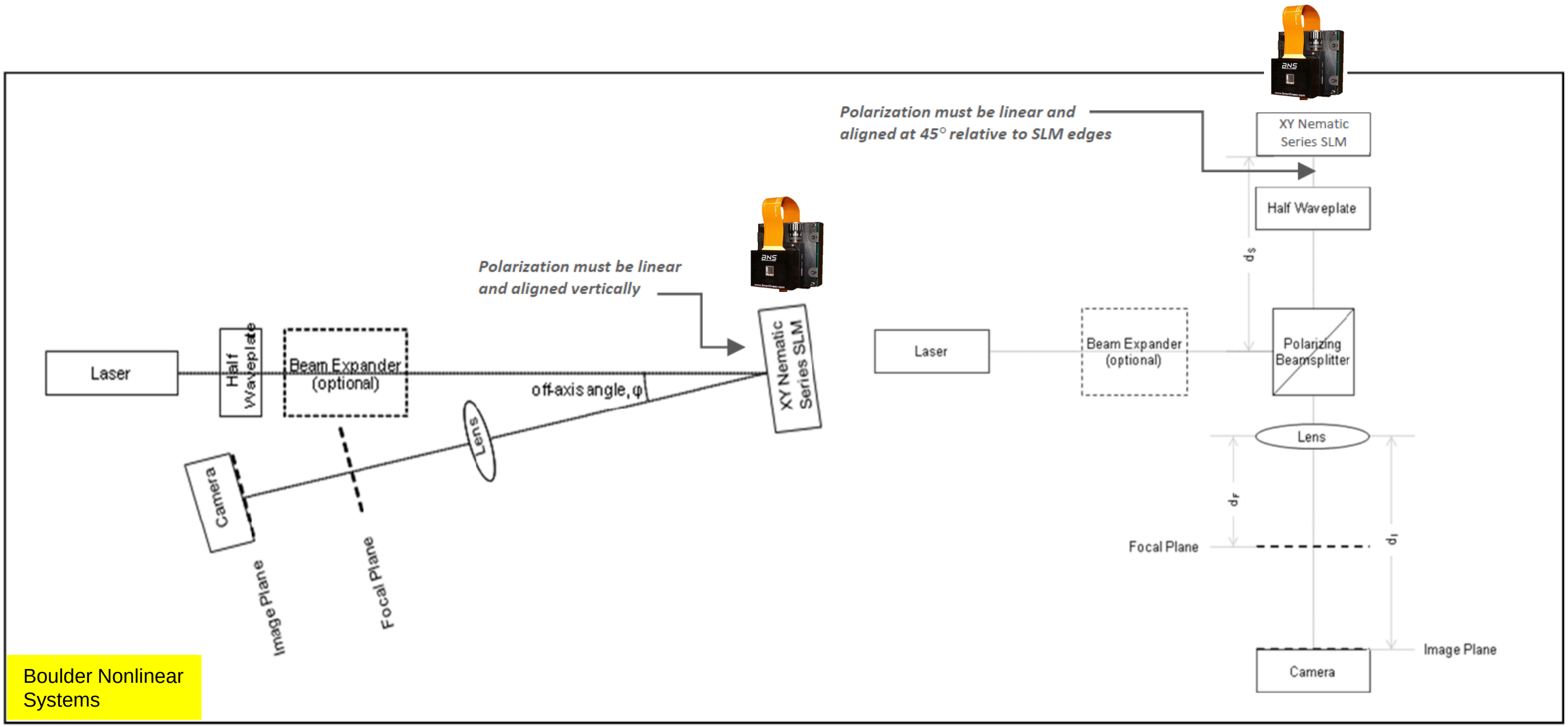

Nematic SLM used for Phase-only Modulation

Nematic SLM used for Amplitude Modulation

Deformable mirror fabrication example: deformable membrane mirror

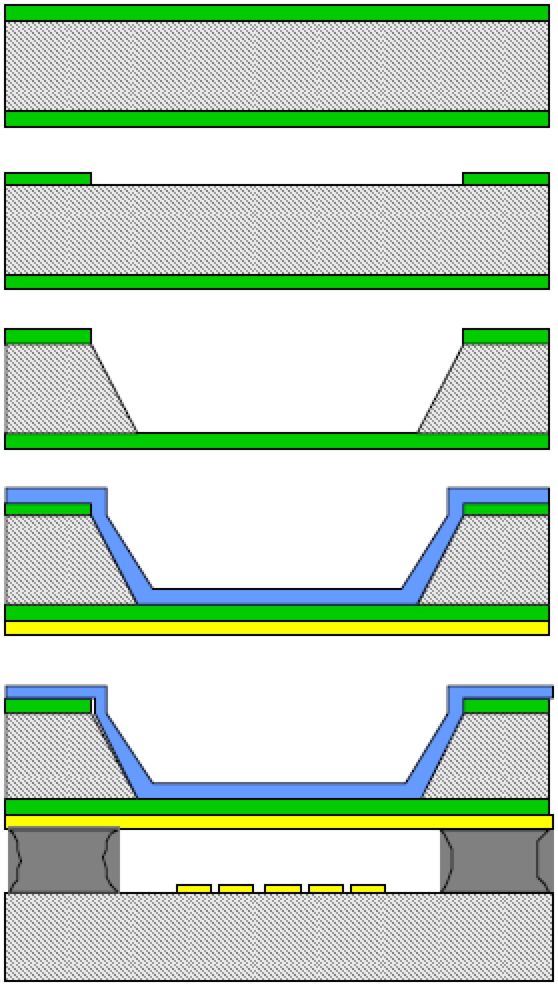

1. Start With Silicon Wafer Coated Both Sides With Low-Stress Silicon Nitride
2. Remove Silicon Nitride in Membrane Area Using Photolithography & Plasma Etch
3. Etch Away Bulk Silicon Wafer Material With KOH To Expose Silicon Nitride Membrane
4. Deposit Reflective Coating On Front of Membrane & Conductive Coating On Back
5. Deposit Conductive Pad Array On Separate Silicon Substrate & Bond to Back Side of Mirror Substrate Using 50 µm Glass Spacer Beads

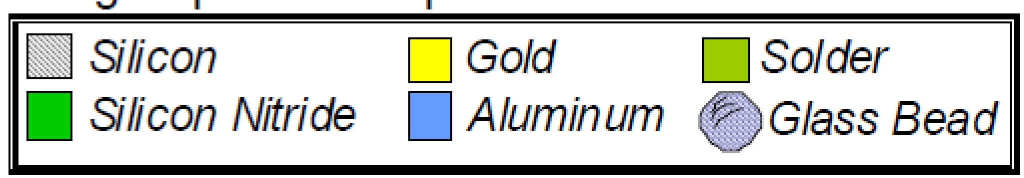

agiloptics.com

Nanolaminate deformable mirrors

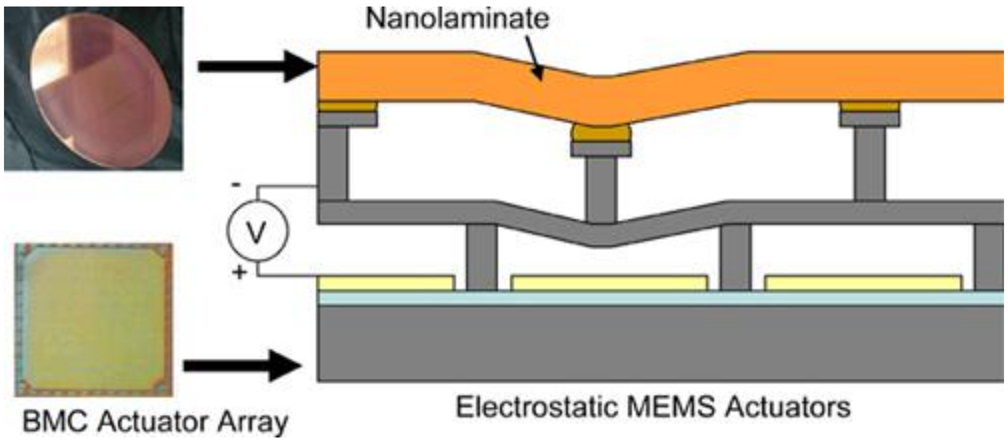

•up to 1 meter possible
•space telescope application

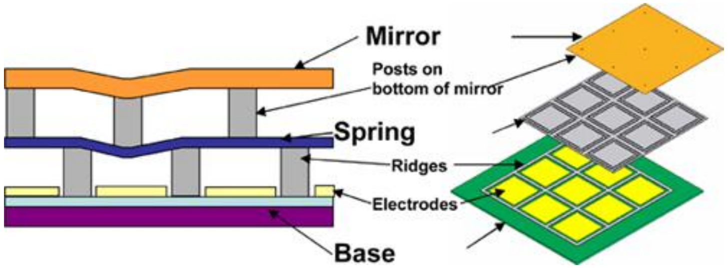

SPIE newsroom 2006
http://spie.org/x8795.xml

Transverse shaping with deformable mirror at SPring8

Structure of DM-Actuator:

Voltage: 0 ~ 255 V

Actuator:

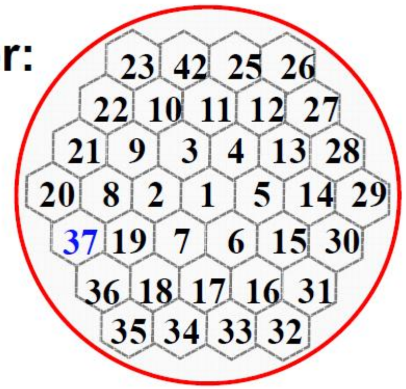

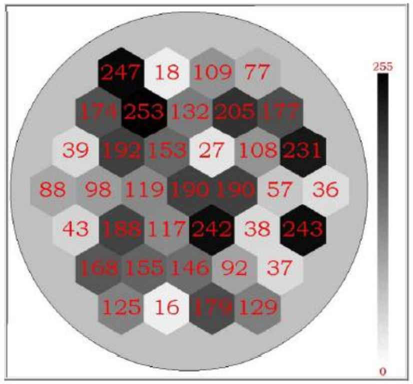

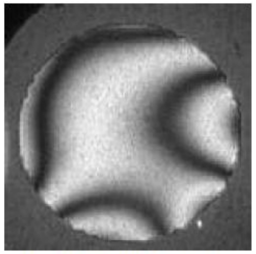

Initial State (All: 0V)

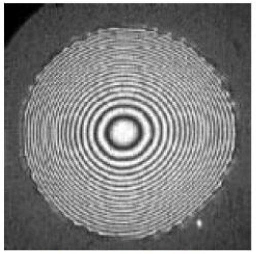

All: 125V

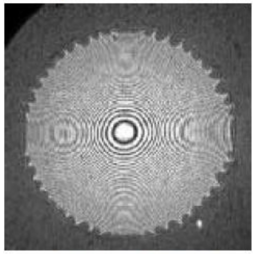

All: 255V (Max. Voltage)

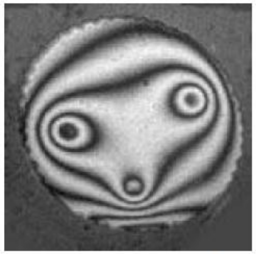

Random Voltage

http://www.okotech.com/

H Tomizawa ICFA 09

Transverse shaping with deformable mirror at SPring8

Cylindrical

Mirror cell: 59
Deformation step: 250 → **Combination: $250^{59} \sim 10^{141}$!**

AI-Algorism for spatial shaping is under development

DM
Double reflection

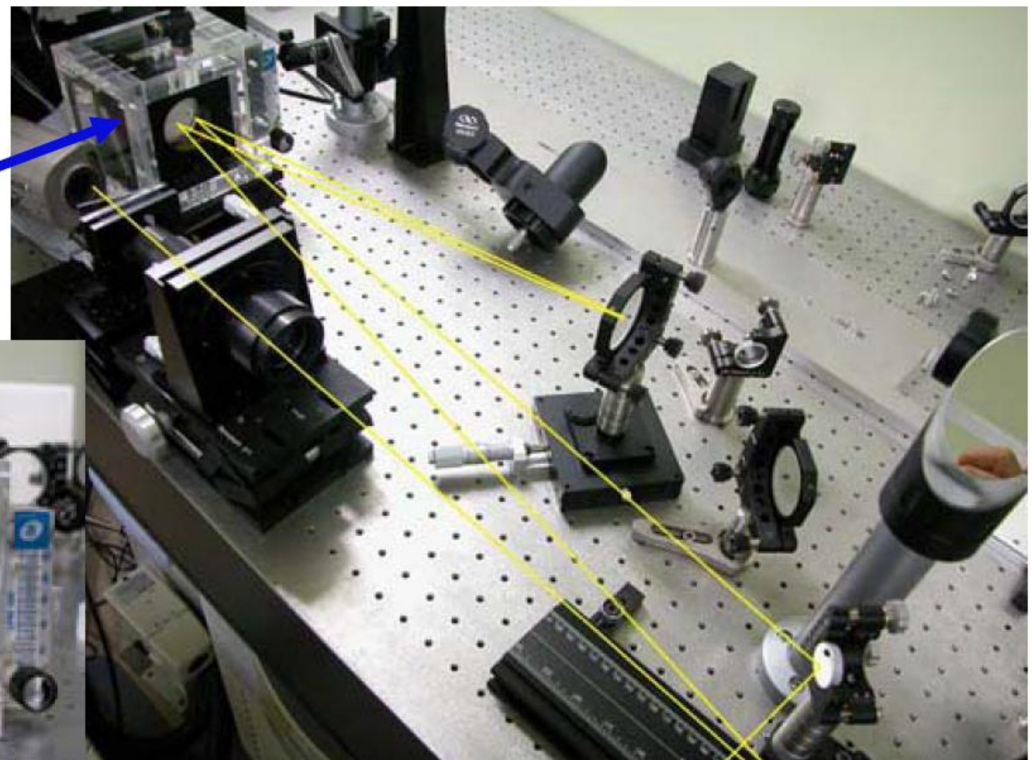

H Tomizawa ICFA 09

Transverse shaping with deformable mirror at SPring8

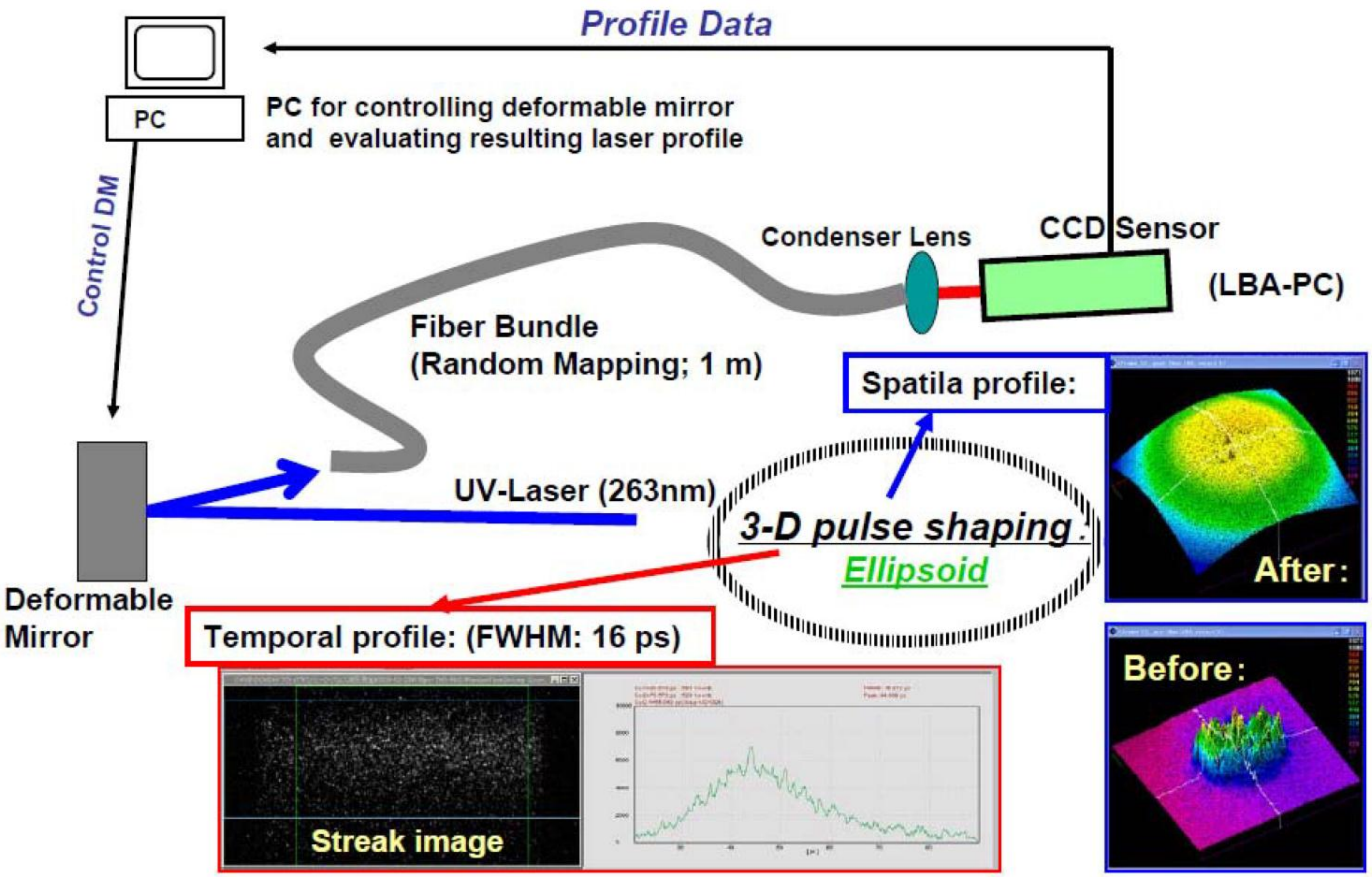

H Tomizawa et al Quant Elec 37, 697 (2007)

Transverse shaping: truncated Gaussian

Gaussian to flat top clipping: PITZ and ATF/DESY

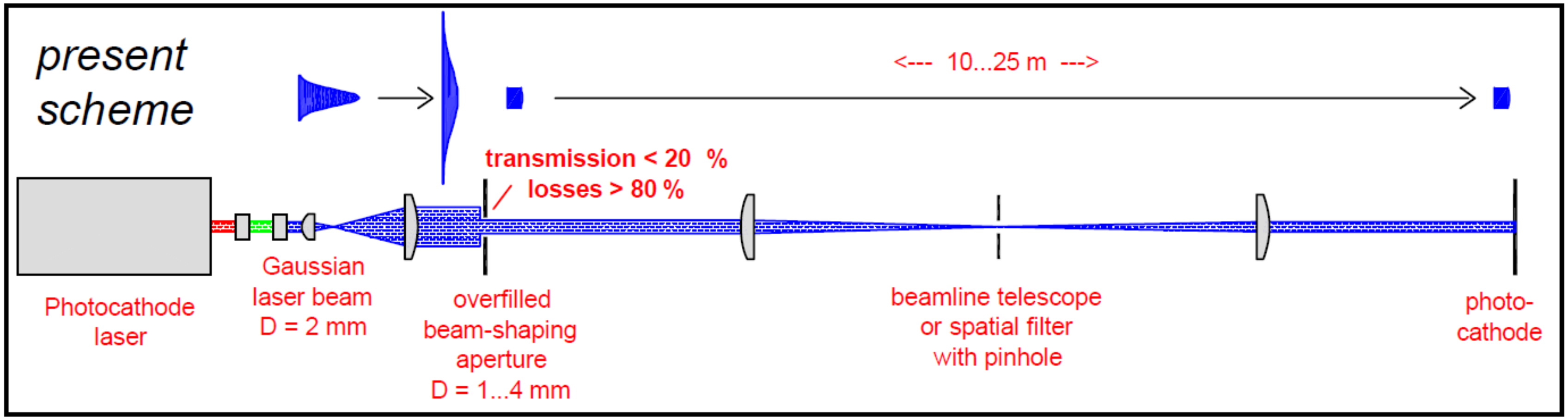

- Imaging the overfilled iris on laser table
- Problem: larger pointing jitter than iris in front of vacuur
- Jitter about 0.5 of diameter min/max

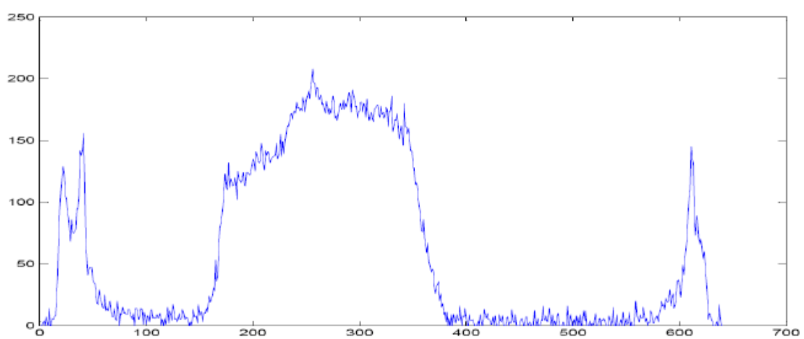

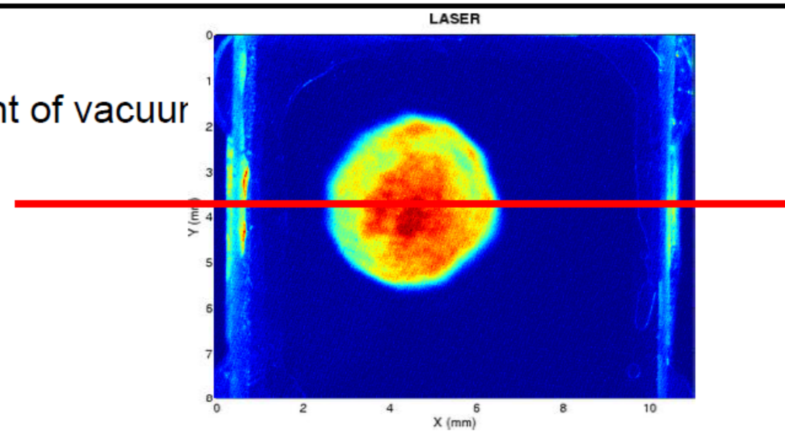

Ingo Will, Max-Born Institute

S. Schreiber, DEZY

PITZ mini pulse shaping workshop, 2007

Yuelin Li 2008 USPAS

Transverse shaping truncated Gaussian, LCLS results: simulations

Distributions after a 1 mm aperture

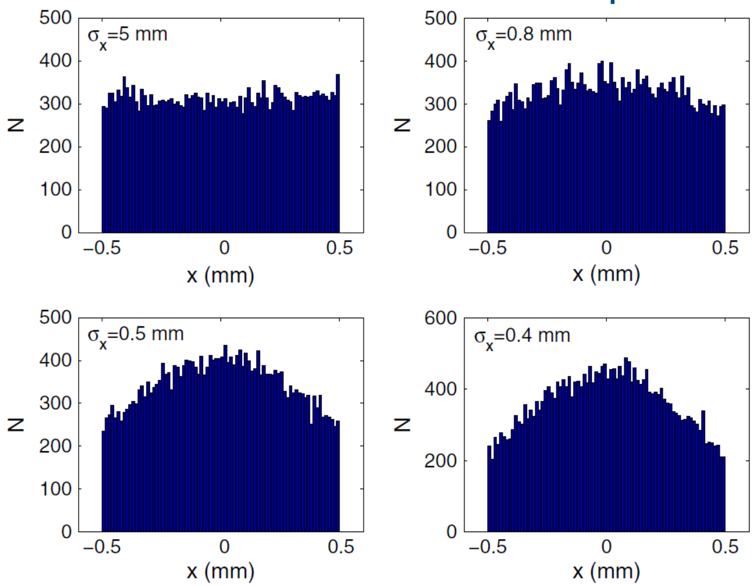

slice & projected emittances

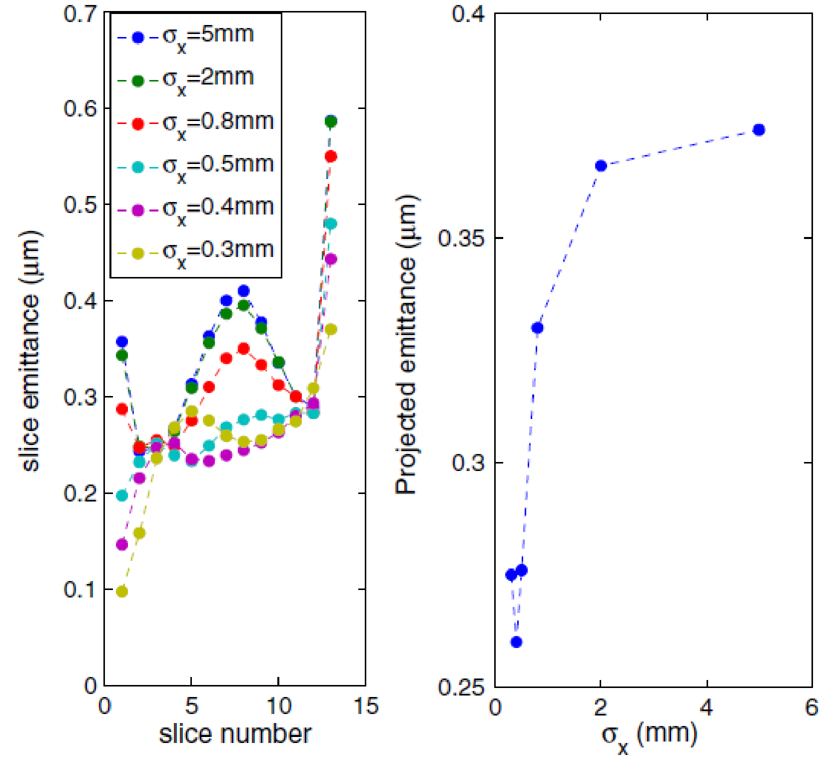

Transverse space charge force

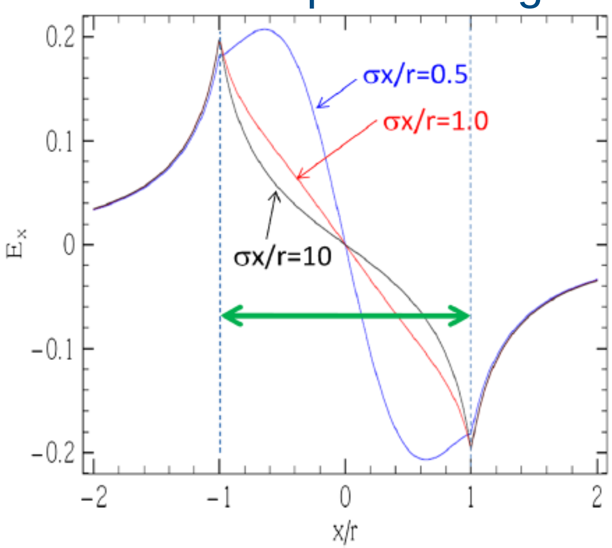

- truncate Gaussians of different rms widths σ_x with an aperture of radius r=0.5 mm. σ_x/r varies from 0.5 to 10
- σ_x = 5 ‘uniform’, σ_x = 0.8 ‘nearly uniform’, smaller σ_x ‘truncated’
- simulations use multiparticle tracking code IMPACTT
- transverse space charge forces more linear across more of aperture and emittances better for truncated beams

Zhou et al. PRST AB 15, 090701 (2012)

Transverse shaping truncated Gaussian, LCLS results: experiment

nearly uniform

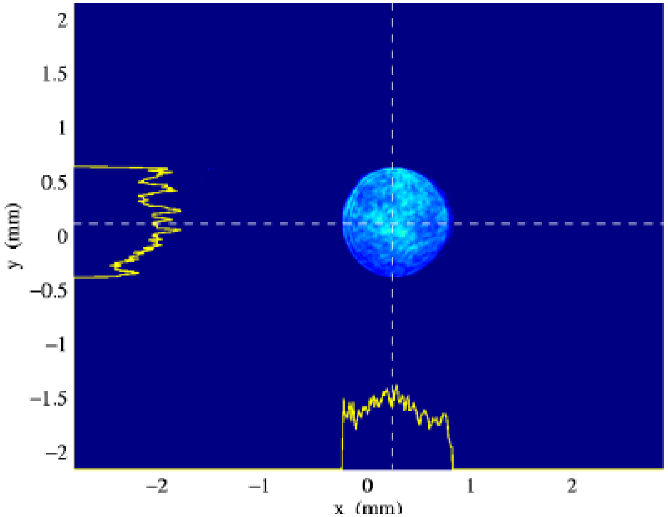

truncated

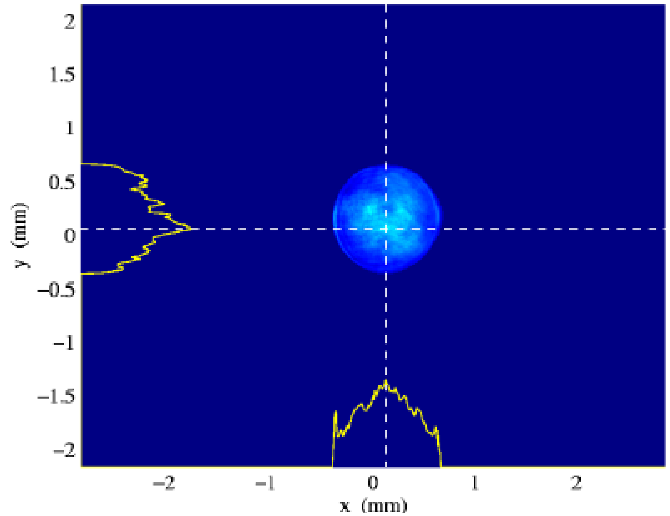

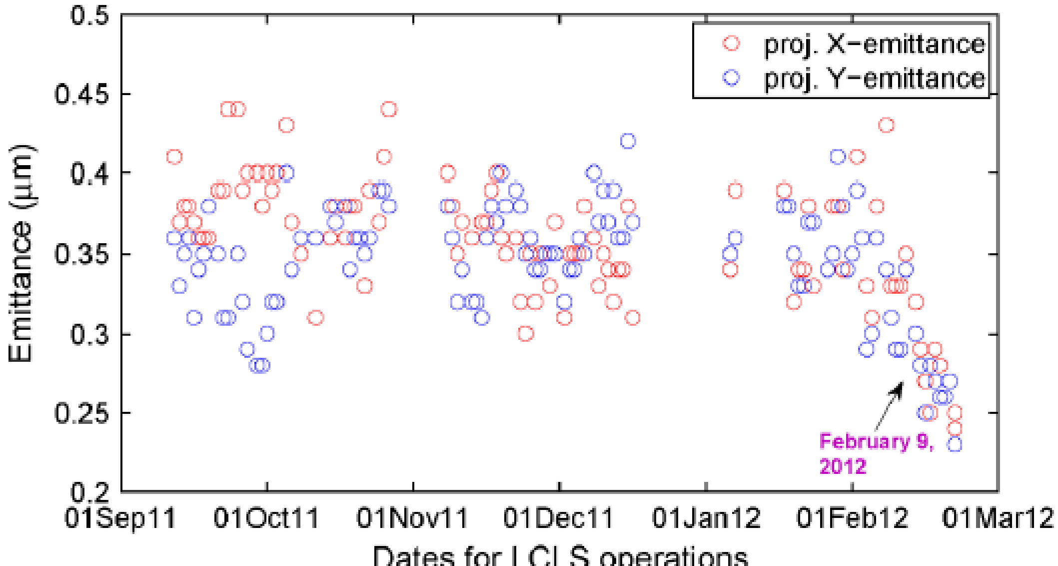

- switched operation (February 9) from nearly uniform to truncated and find on average a 25% reduction in emittance
- increased optical transmission through the aperture 2x.

Zhou et al. PRST AB 15, 090701 (2012)

Transverse shaping, earlier LCLS study

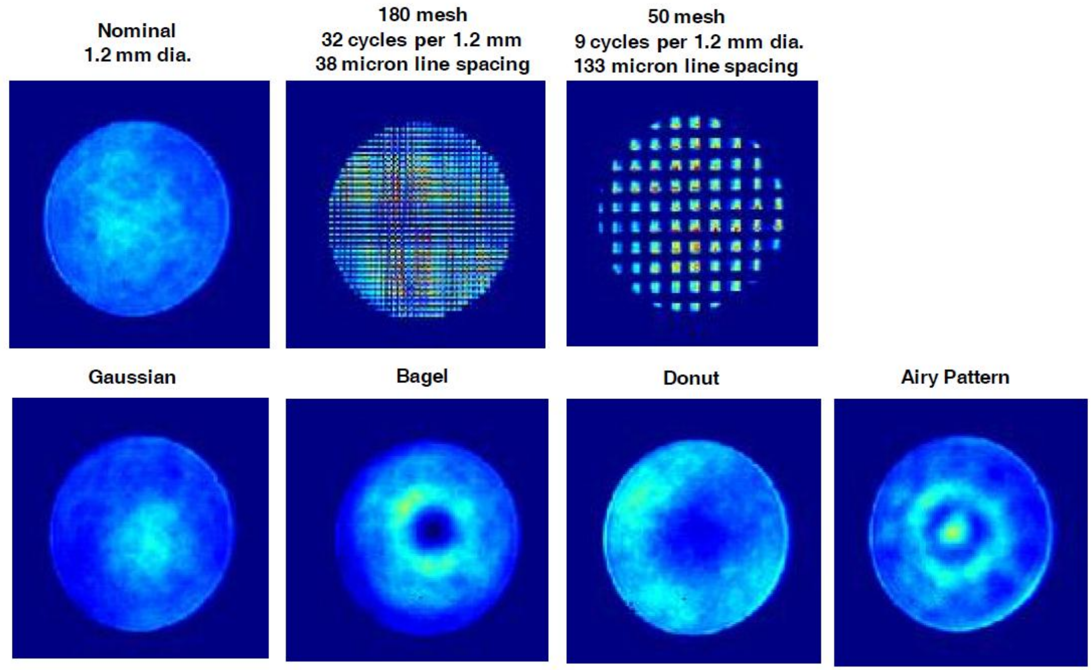

Figure 1: (color) The seven laser shapes used in the electron beam and FEL lasing studies. The edge diameter of all the shapes is 1.2 mm.

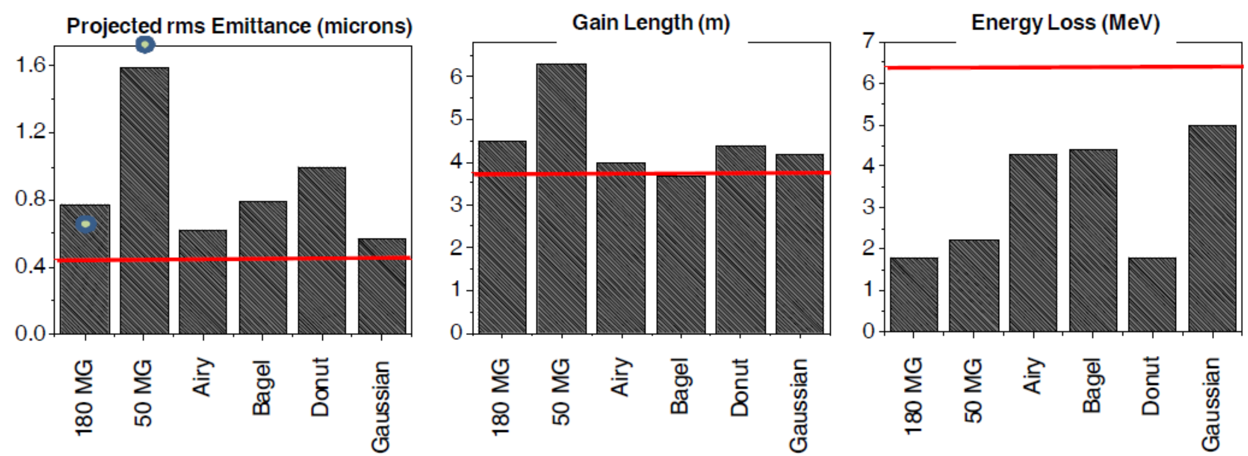

Brachmann et al, FEL 2009 proceedings WEOA03 (p. 463)

Fourier Transform Temporal Shaping

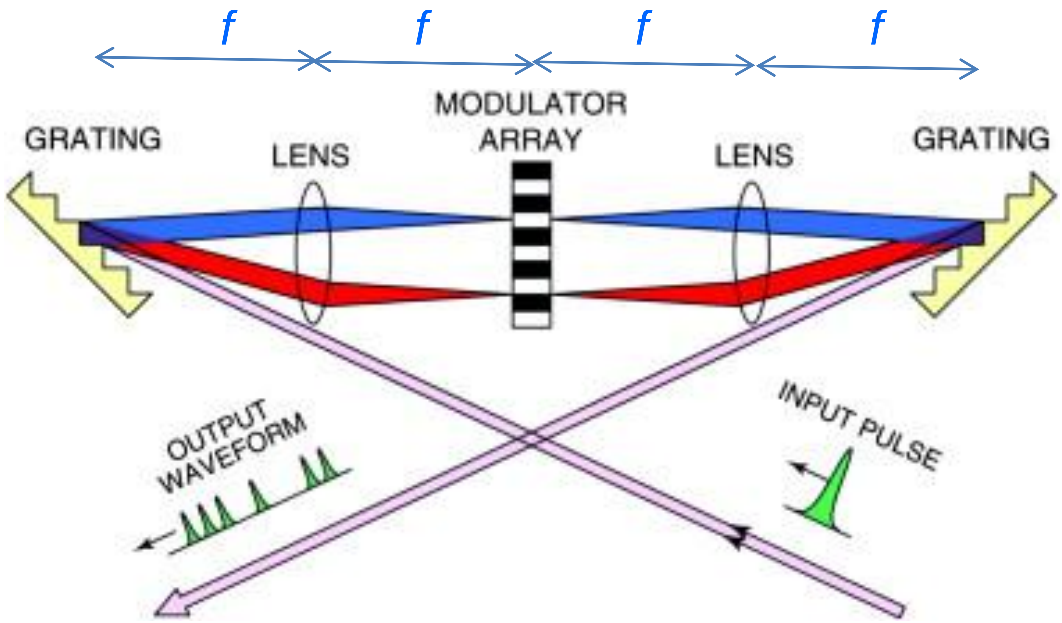

Basic setup for Fourier transform optical pulse shaping.

- Recall the grating stretcher
  - here gratings are a distance f from the lenses – 0 length stretcher
    - separating the frequencies in the focal plane without introducing any path length difference
  - grating 1 maps freq->angle, lens 1 maps angle->position; after modulation, lens 2 and grating 2 invert the maps.
- Modulator array can alter both intensity and phase of addressable frequency components

AM Weiner Opt Comm 284, 3669 (2011)

Fourier Transform Temporal Shaping

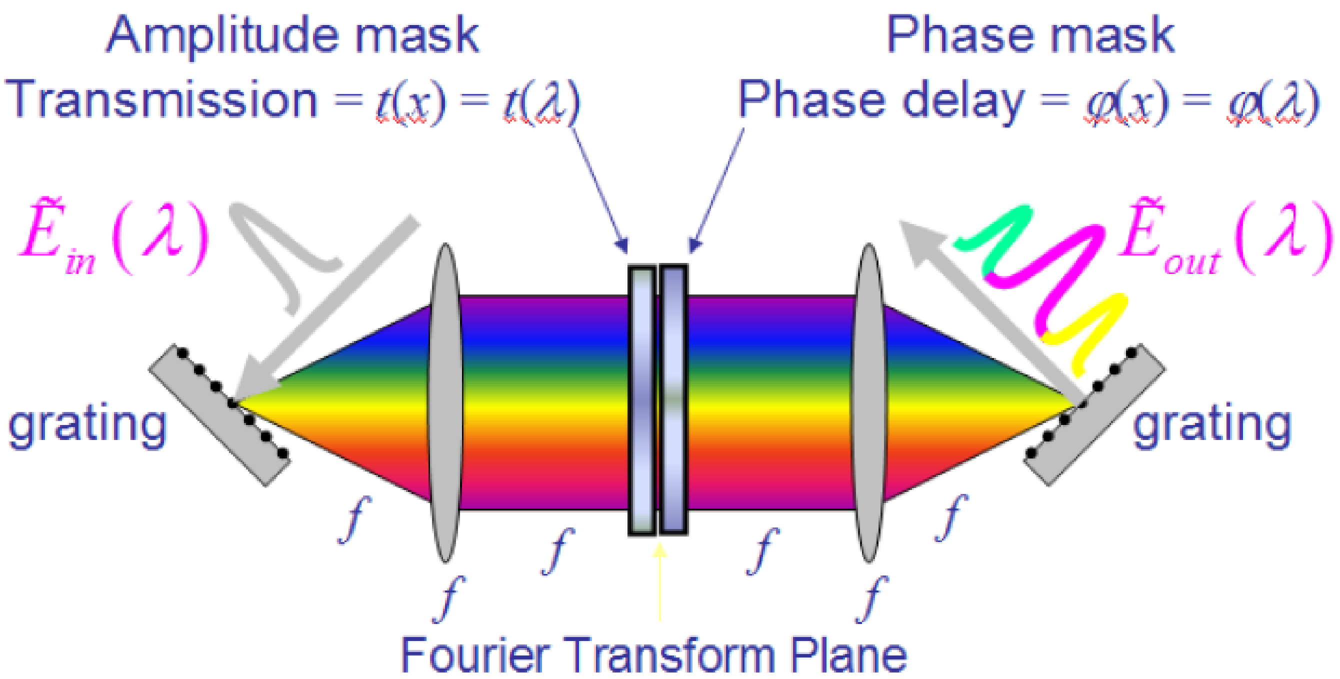

R. Trebino

$$H(\lambda) = t(\lambda)\exp[i\varphi(\lambda)]$$

• Modulator array can alter both intensity and phase of addressable frequency components

•eg 2 SLMs & 2 polarizers

• multiply by transfer function and transform back to time domain to obtain temporal pulse shape

FT shaping examples

spectra of ideal square pulse & ion-etched mask

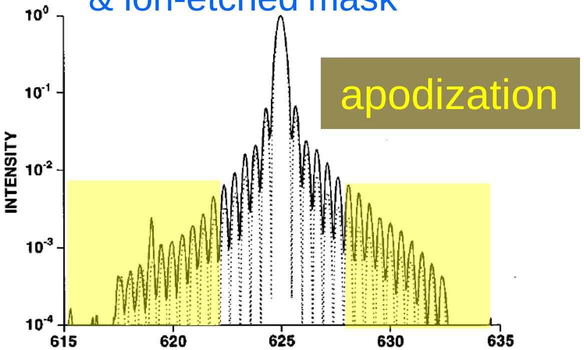

measured

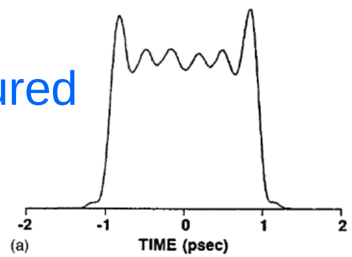

theory

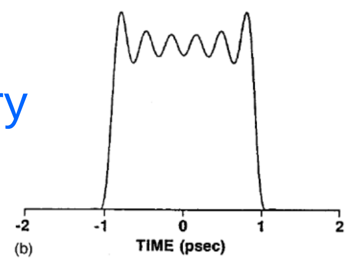

measured with softer apodization

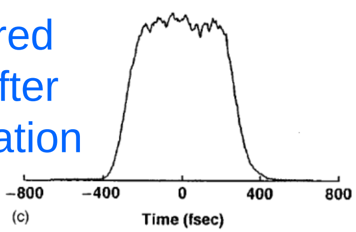

Pseudorandom bit sequence using phase modulation only

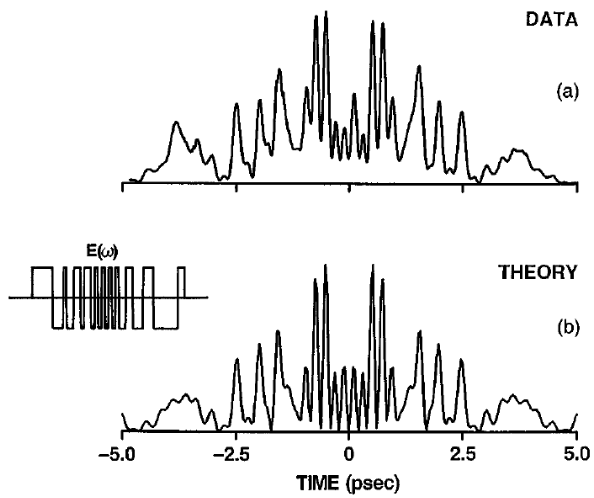

fixed mask with central frequency blocked

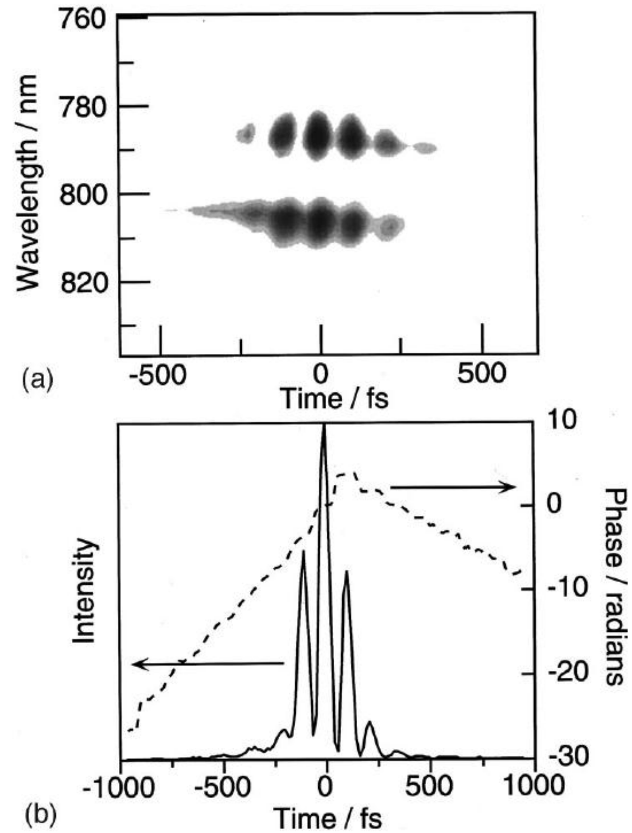

AM Weiner Rev. Sci. Instrum., Vol. 71, No. 5, May 2000

Using an AOM as a modulator

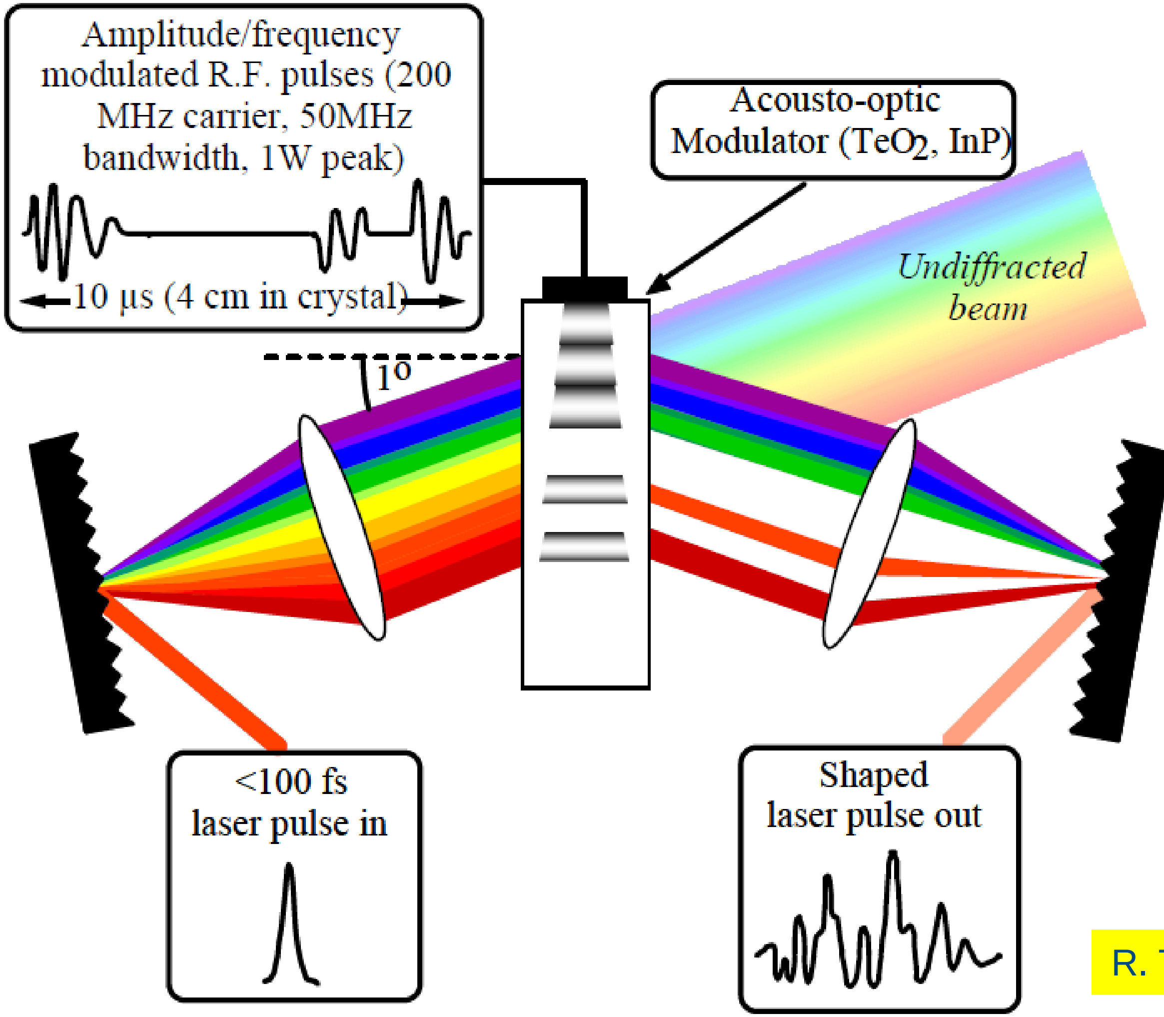

- transmission is lower, due to using diffracted wave
  - often doesn't matter if pulse is subsequently amplified
- much higher frequency resolution
- continuous modulation (no hard pixel boundaries)

R. Trebino

Acousto-optic programmable dispersive filter (AOPDF, Dazzler)

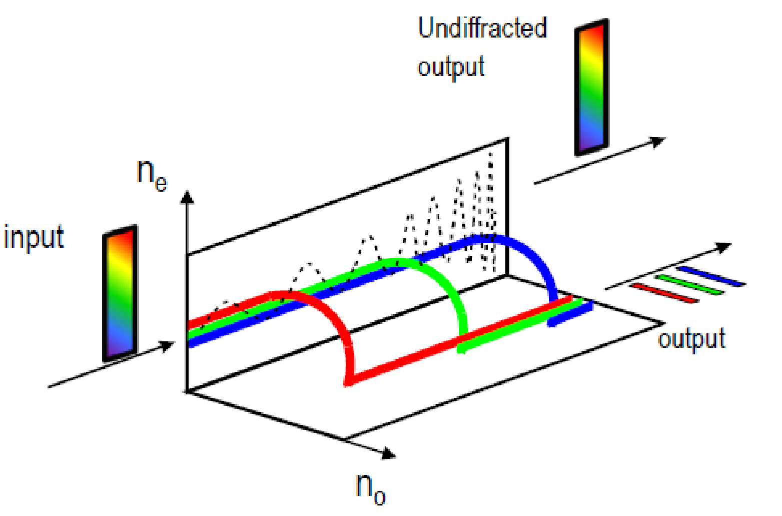

C. Vicario EPAC 04

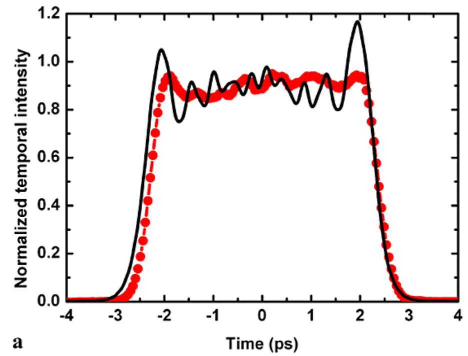

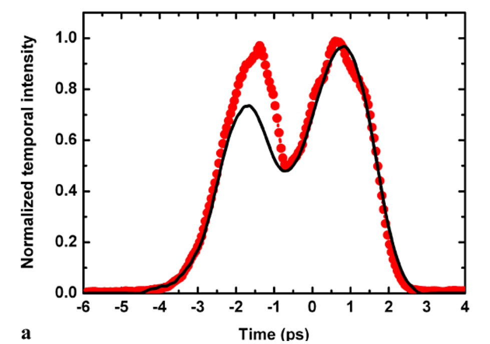

Pulses shaped directly in the UV using stretcher + UV AOPDF at PSI. red measured, black theory

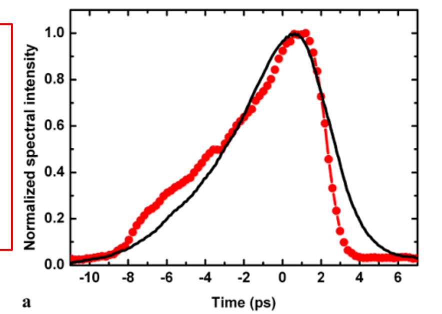

- wavelength-selectively scatter between e- and o-wave using RF-generated acoustic wave
- continuous modulation, no pixel boundaries
- high bandwidth -> high wavelength resolution
- can now work directly in UV (less resolution than IR)
- low efficiency (~20%)
- damage threshold (10's MW peak power)
- length-limited; need pre-stretching for τ > 4ps

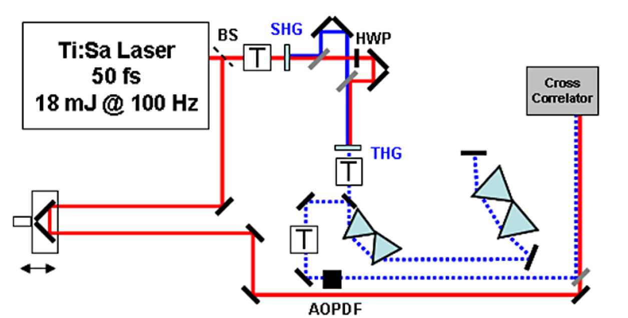

Tisorio et Appl Phys B 105, 255 (2011)

Pulse Stacking

$$\sum_{n=0}^{15} e^{-2\left(\frac{t-n\delta}{\tau}\right)^2}$$

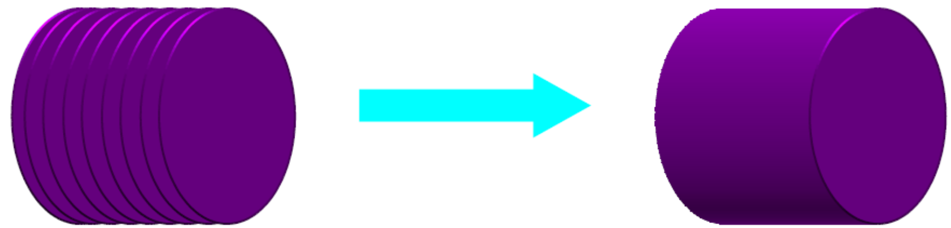

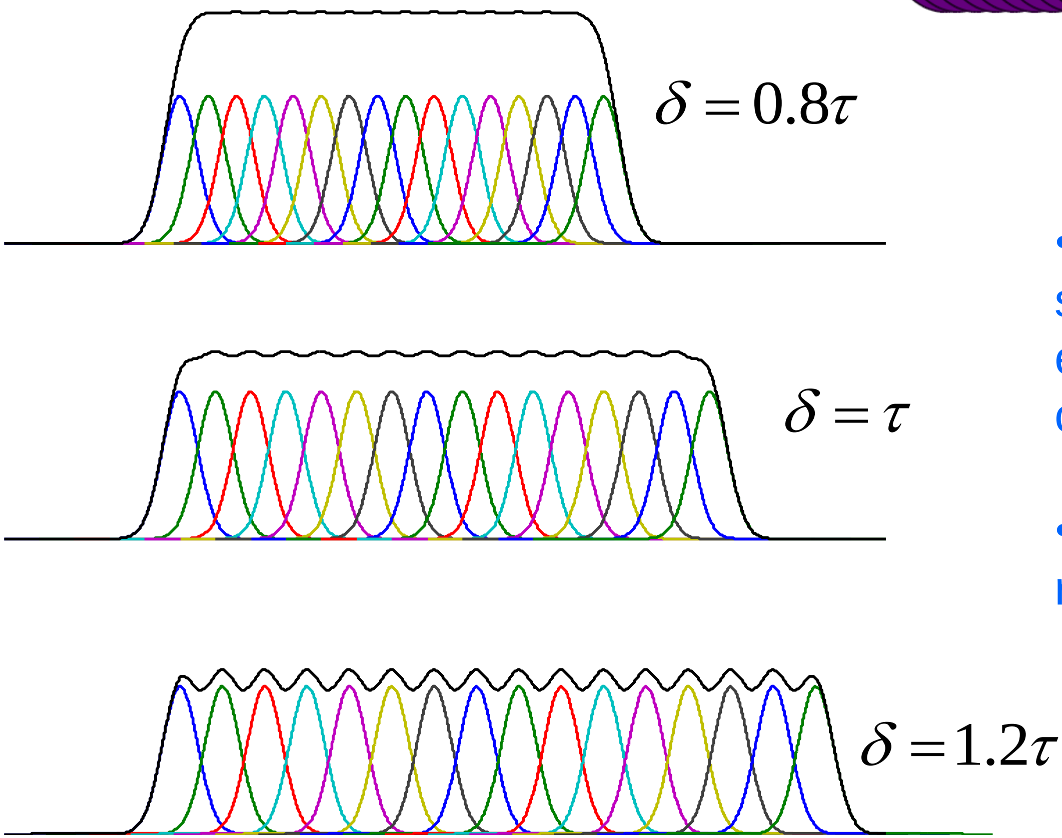

- Summing multiple pulse replicas shifted in time, closely separated enough that they merge into one continuous pulse

- Gaussians give flat top with little ripple for $\delta < \tau$

First ultrafast incarnation, ca 1998

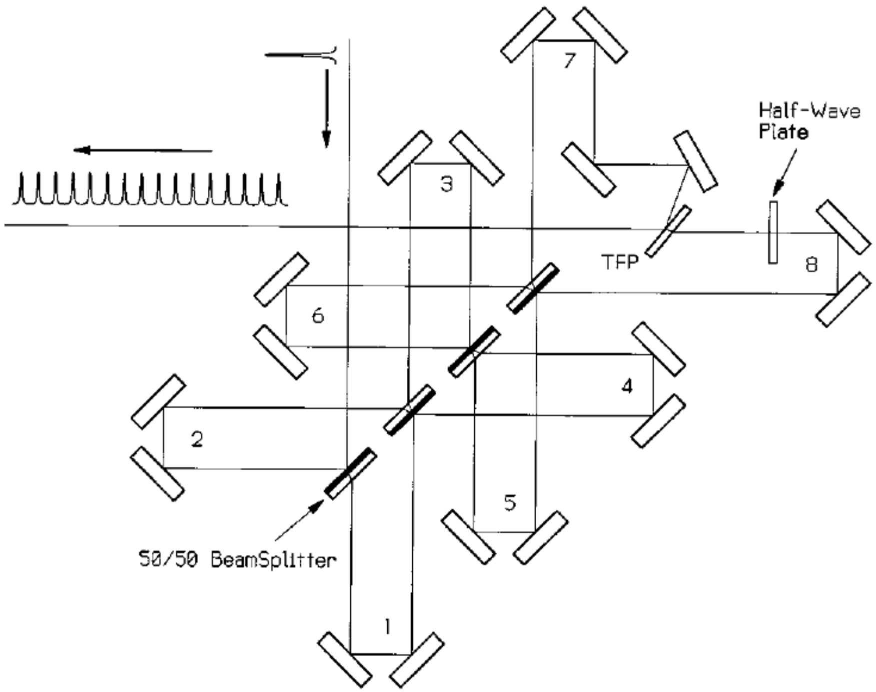

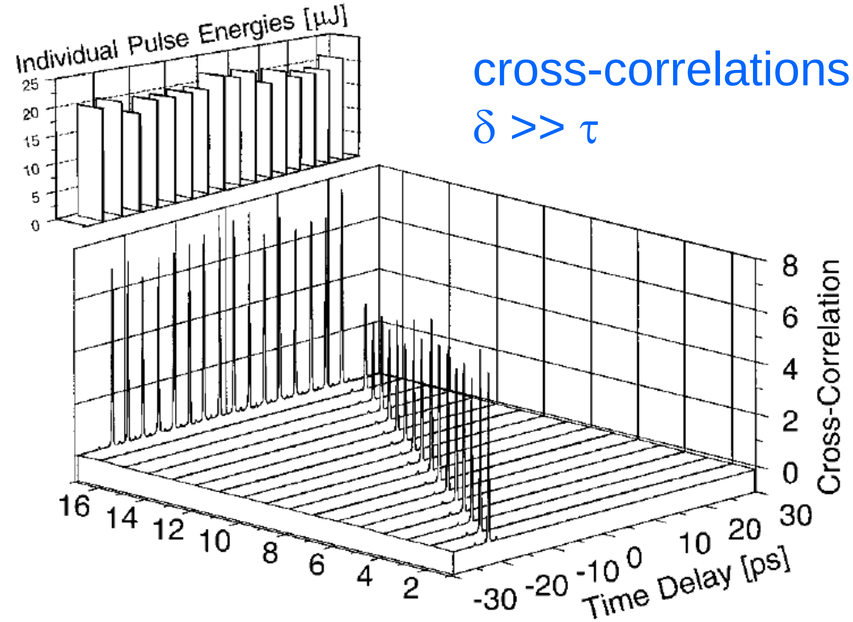

cross-correlations
$\delta >> \tau$

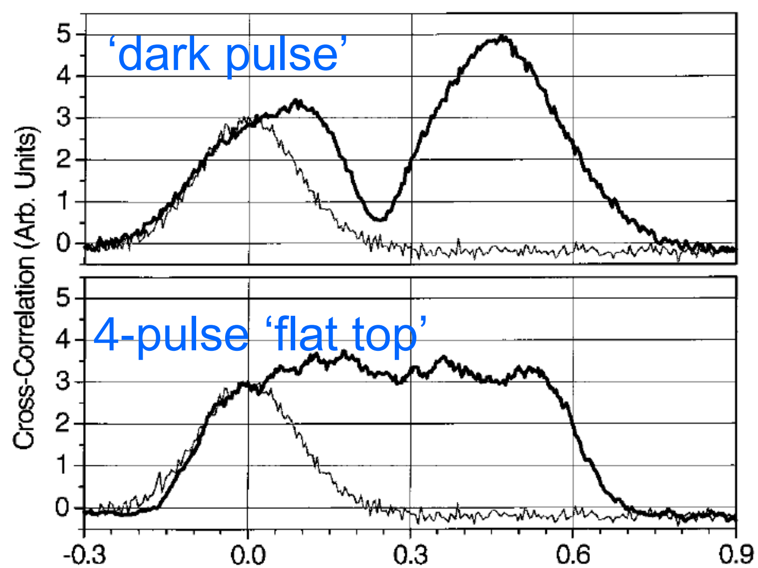

- Dielectric beamsplitters, 1st 8 pulses polarized orthogonal to last 8
  - adjacent pulse interference
- can't balance intensities
- alignment nightmare

Siders et al Appl Opt 37, 5302 (1998)

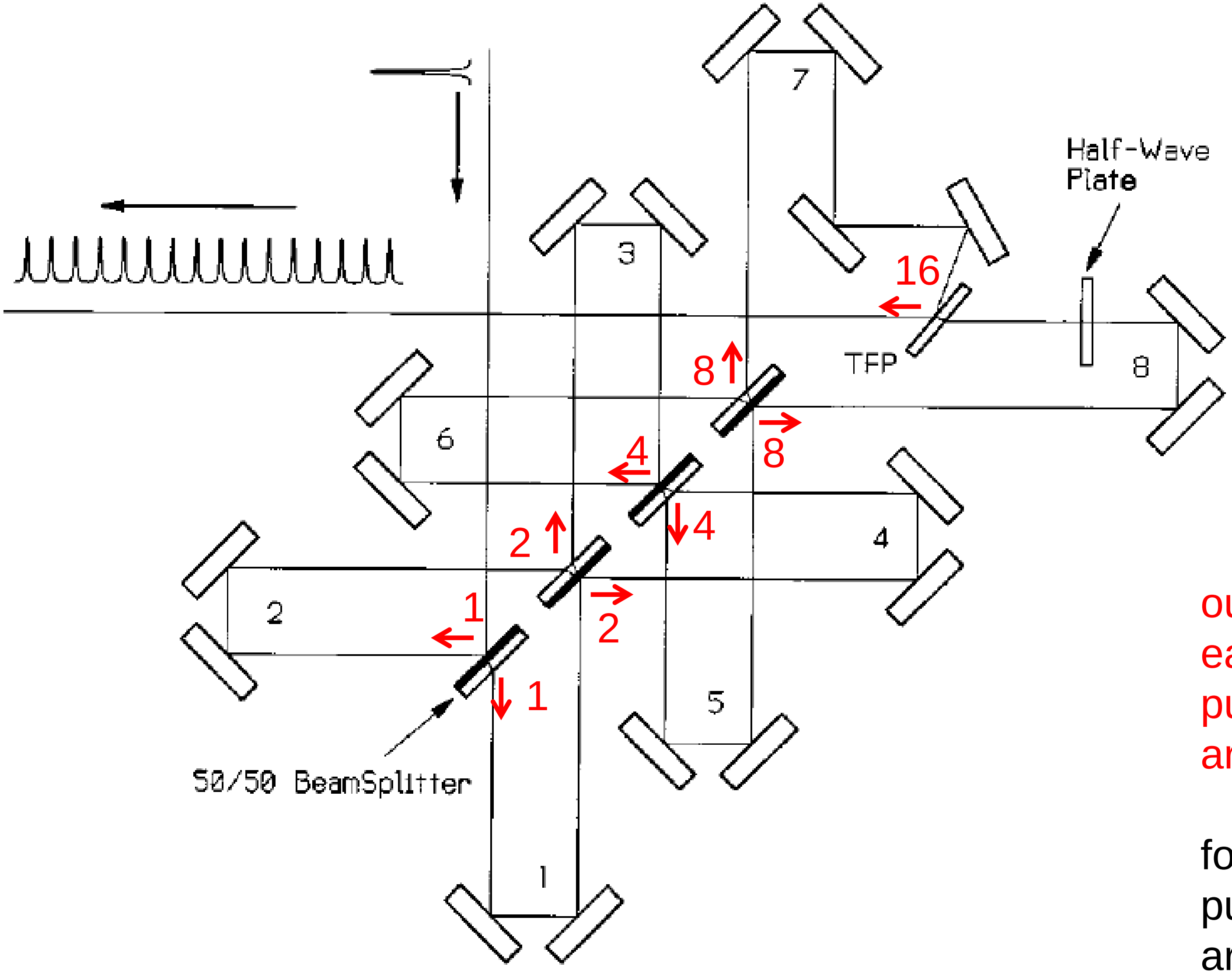

output directions at each splitter and # of pulses in each output are marked in red

for equally spaced pulses, arms 2,3,6 & 8 are 0.5δ, δ, 2δ, and 4δ longer than arms 1,4,5, &7

Spring8 implementation

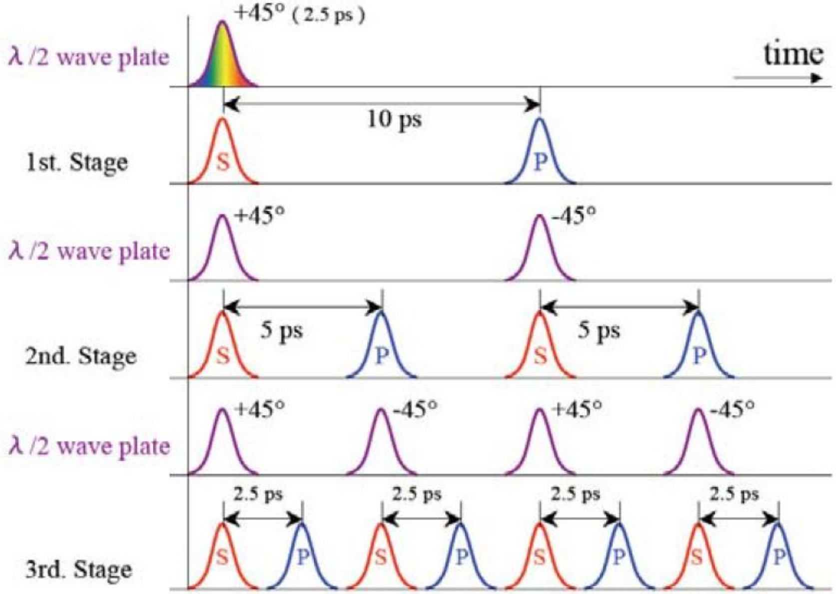

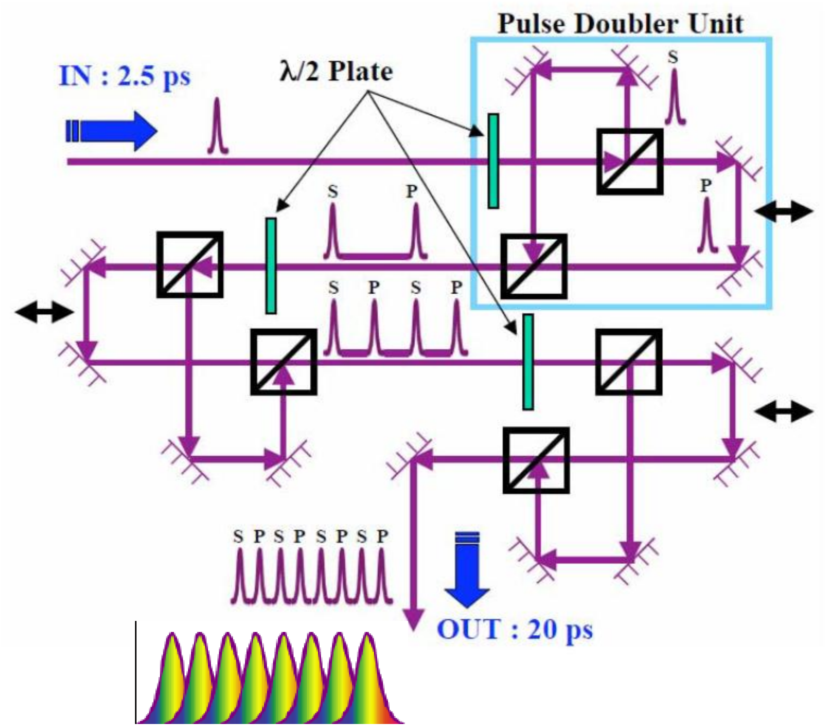

- start with 100 fsec pulse, chirp with Dazzler to 2.5 psec
- rotate polarization 45 degrees between each doubler unit
- stacked pulses alternate polarization
    - chirp & polarization reduce interference
- can balance intensities with waveplates

H Tomizawa et al Quant Elec 37, 697 (2007)

Birefringent pulse stacking

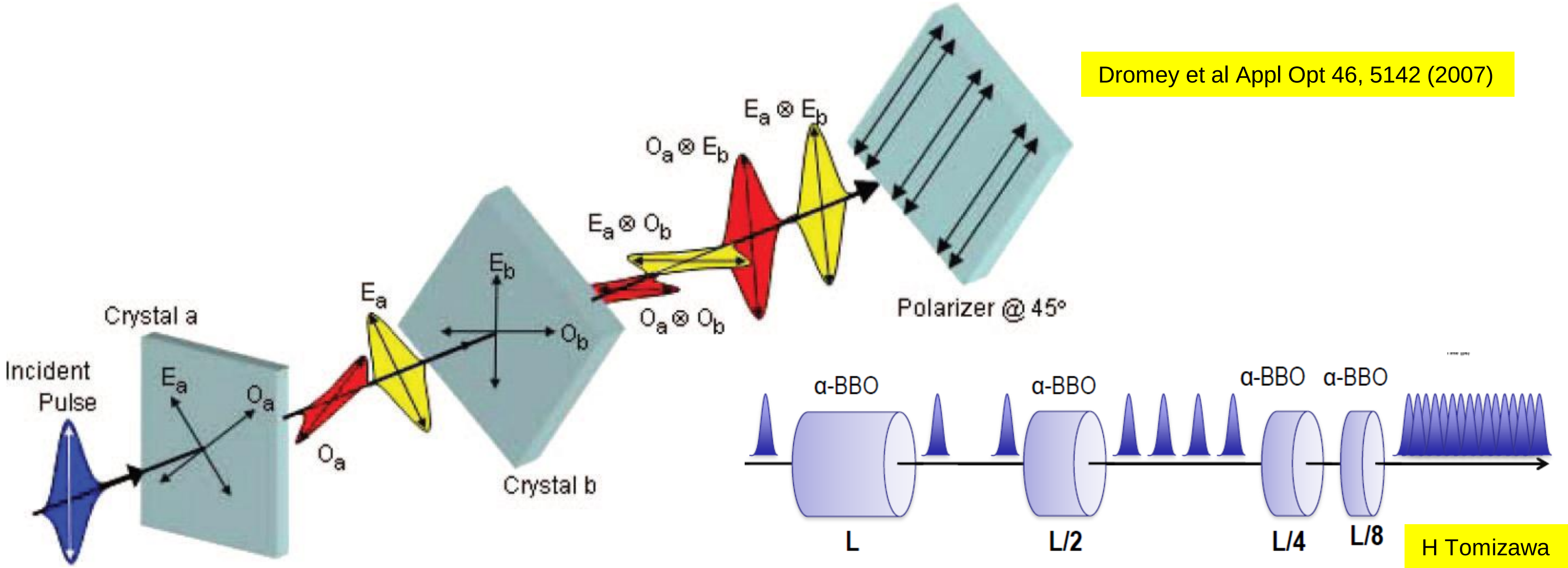

- rotate fast and slow axes 45 degrees after each step
- group velocity different for o and e waves, $\delta = \frac{L}{2^n}\left|\frac{1}{v_o} - \frac{1}{v_e}\right|$
- # of pulses doubles in each crystal
- for equally spaced pulses, tailor crystal lengths to be *L, L/2, L/4,…*
- much more robust alignment
- adjusting δ requires changing crystals
- pulse traverses a lot of material (optical homogeneity, dispersion)

Superstacker

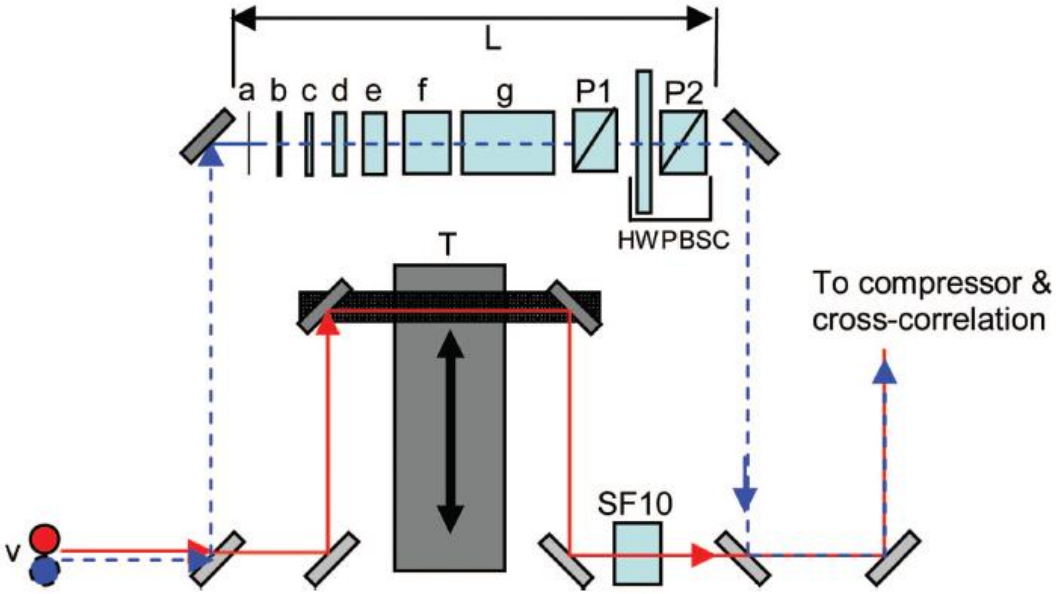

- 128 pulse train
- 40 fsec Ti:Sapph Astra laser at Rutherford Appleton
- 800 nm; Calcite crystals
- cross-correlate with initial pulse

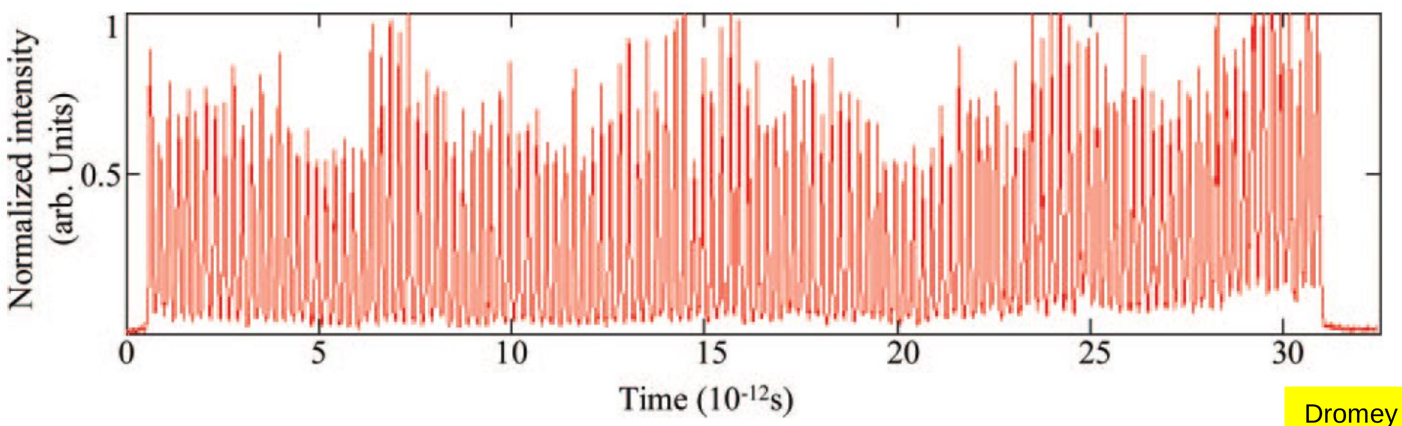

Dromey et al Appl Opt 46, 5142 (2007)

Homework

The group velocity mismatch between *o* and *e* waves in Calcite is 575 fsec/mm at λ=800 nm. Design a stacker to make a top-hat profile 13 psec FWHM from Gaussian pulses that are 1.18 psec FWHM (τ=1 psec in $\exp(-2t^2/\tau^2)$). What pulse pattern do you get from the remaining crystals if you remove each crystal from the stack in turn? Qualitatively, what happens if you try to use the same stacker with pulses of the same width at 532 nm?

(red is ordinary)

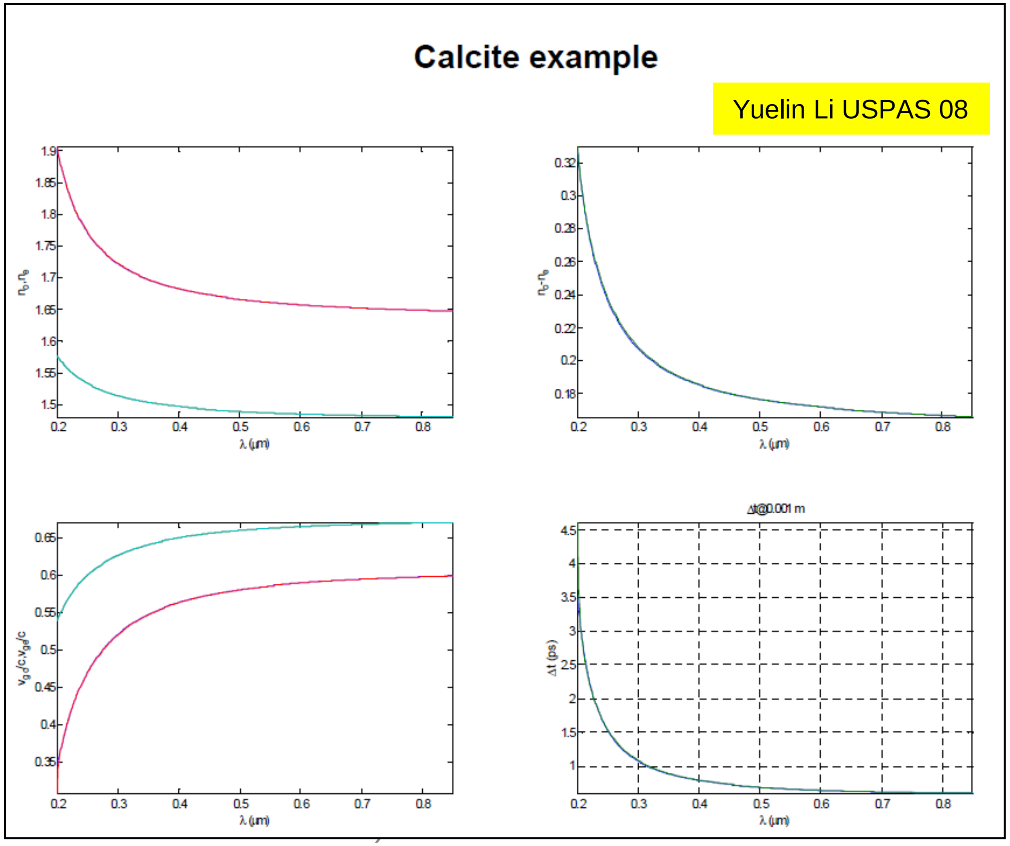

Cornell pulse stacking & e-beam measurements

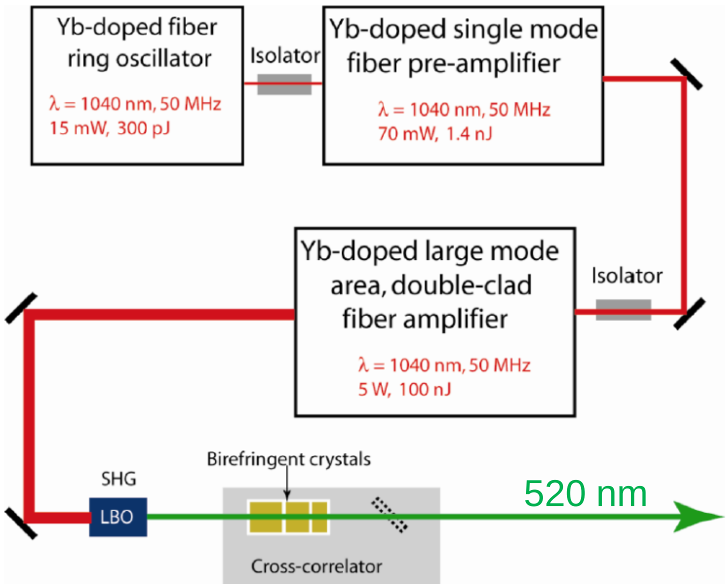

•up to 16-pulse stacker using YVO_4 crystals δ = 1.8, 3.6, 7.2 & 14.4 psec

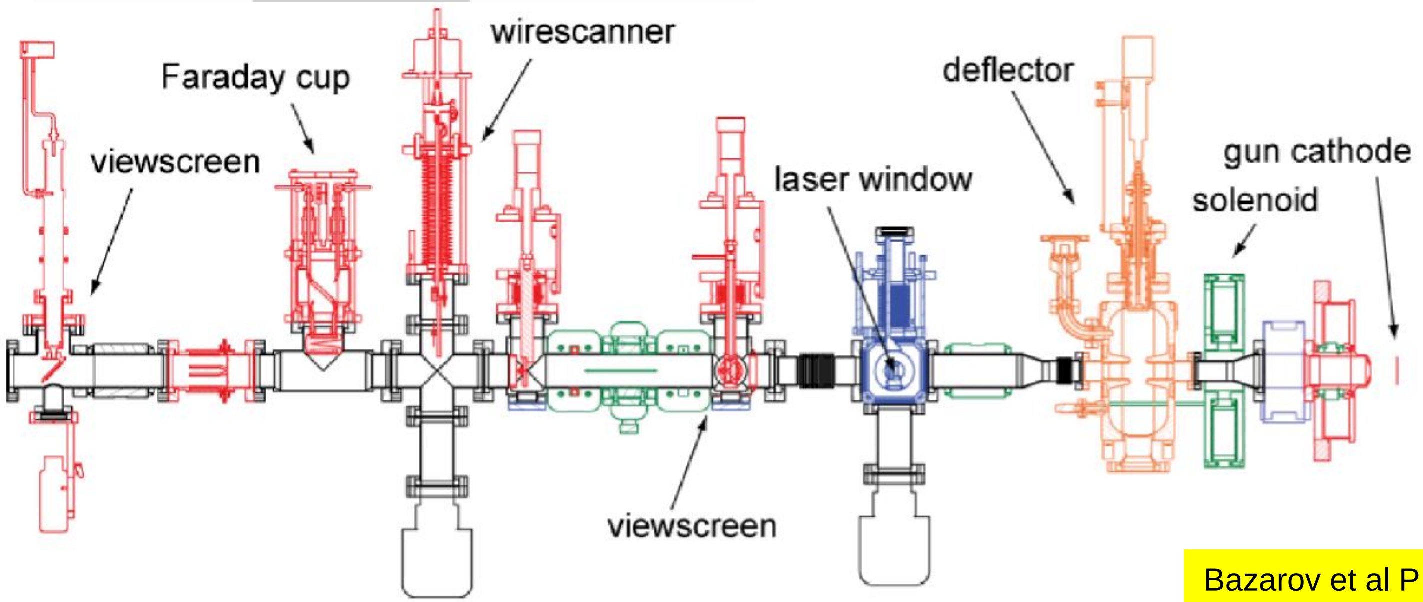

Bazarov et al PRST AB 11, 040702 (2008)

FIG. 1. (Color) Beam line used for temporal profile measurements. Beam direction is to the left.

Cornell results cont.

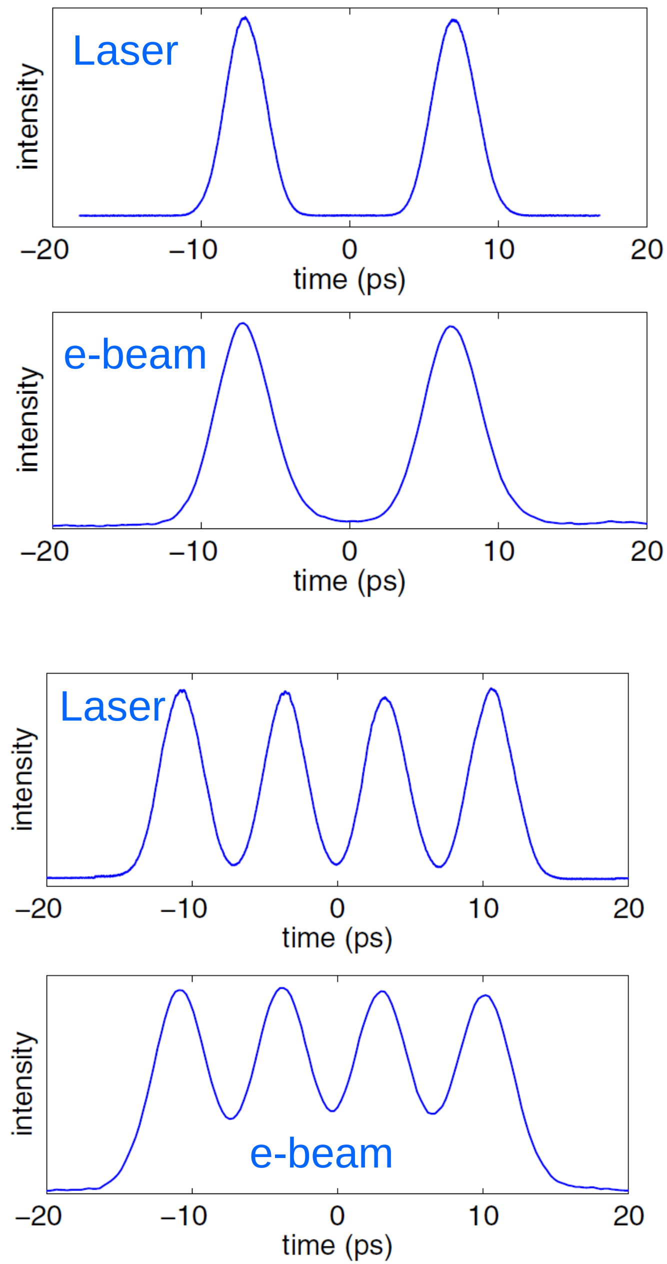

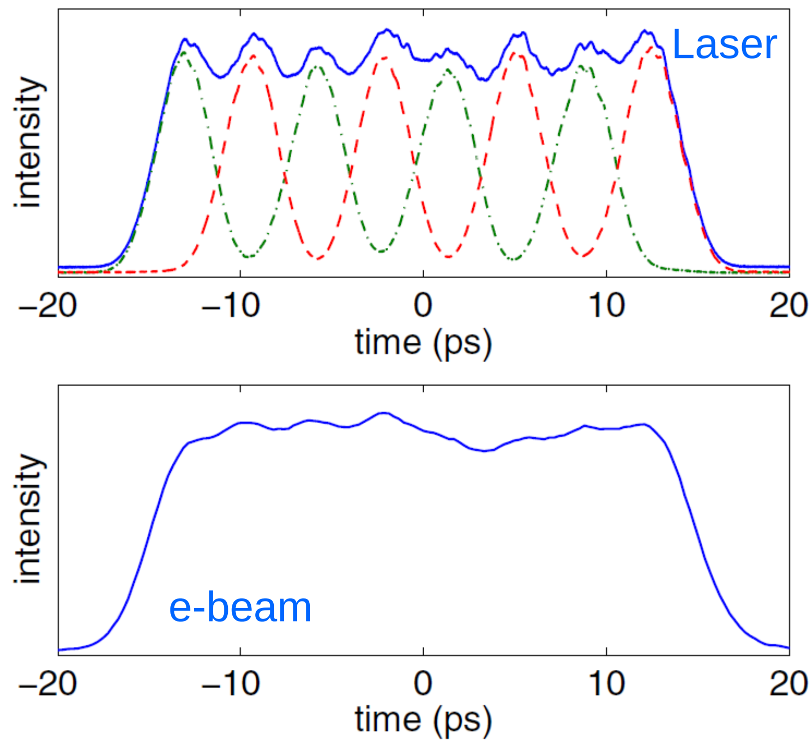

effect of 4th crystal was below the resolution (1.5 psec) of e-beam measurement system

Spring8 results

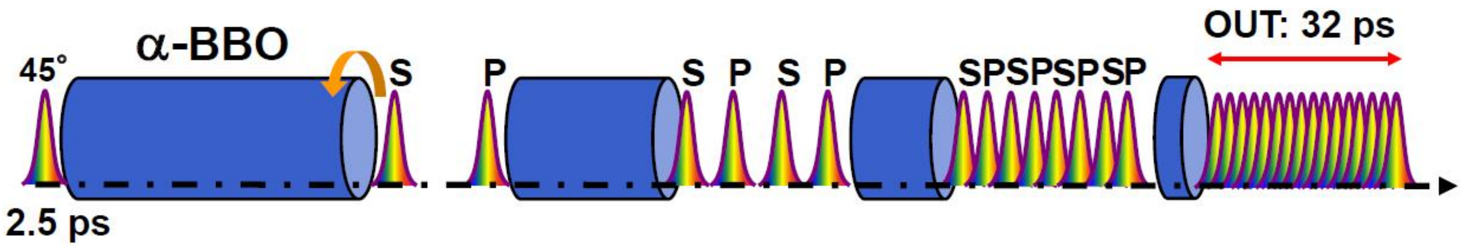

32-ps Square Pulse: *16 pulse stacking*

16-ps Square Pulse: *8 pulse stacking*

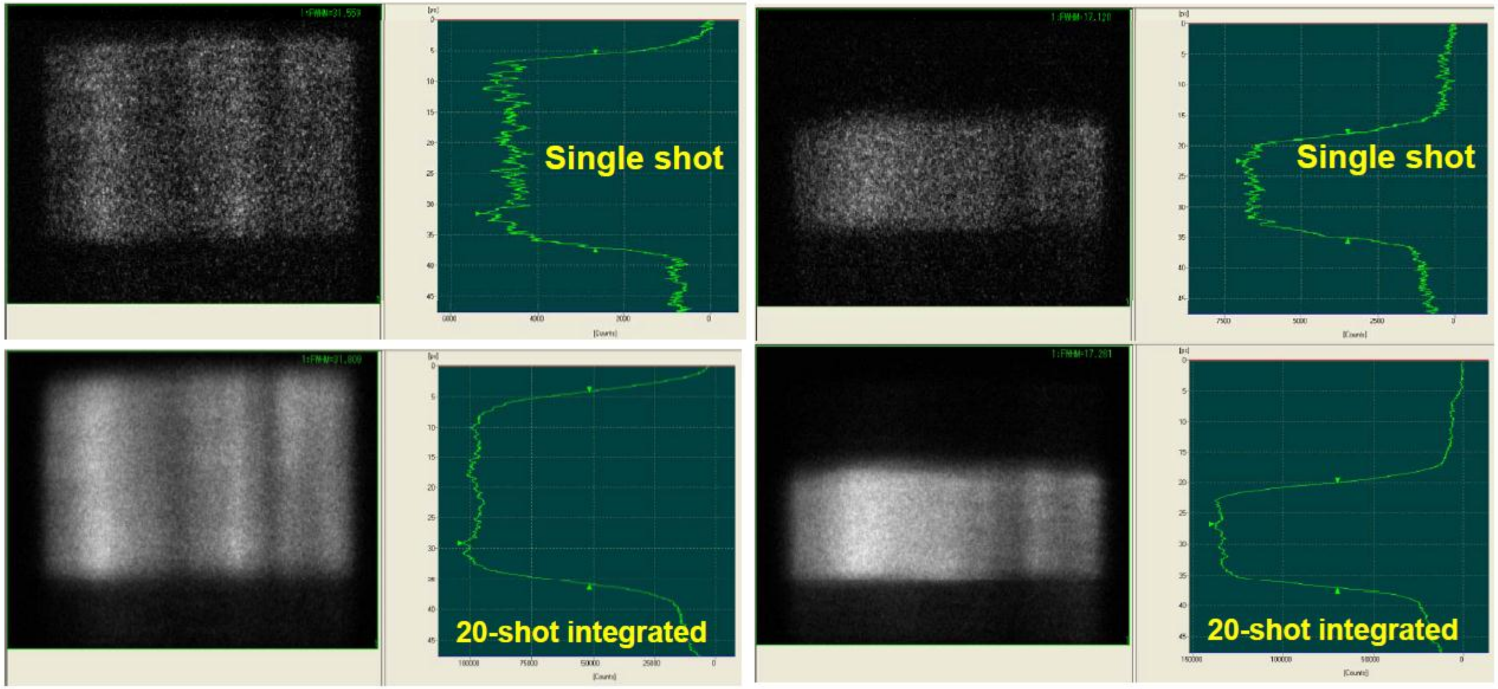

Streak camera measurements

H. Tomizawa ICFA 09

Cornell stacked soliton pulses 3-d measurement

- used Y. Li & J. Lewellen 1st order cross correlation technique for 3-d measurements
- 2-crystal stacker – 4 pulses

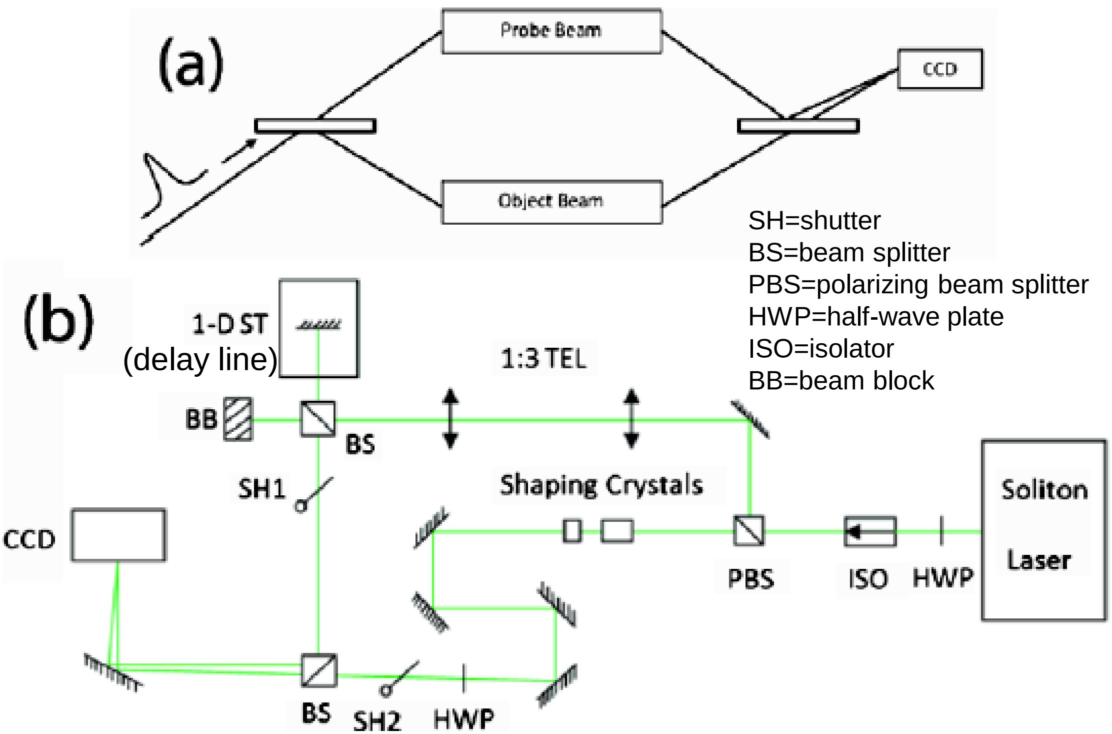

SH=shutter
BS=beam splitter
PBS=polarizing beam splitter
HWP=half-wave plate
ISO=isolator
BB=beam block

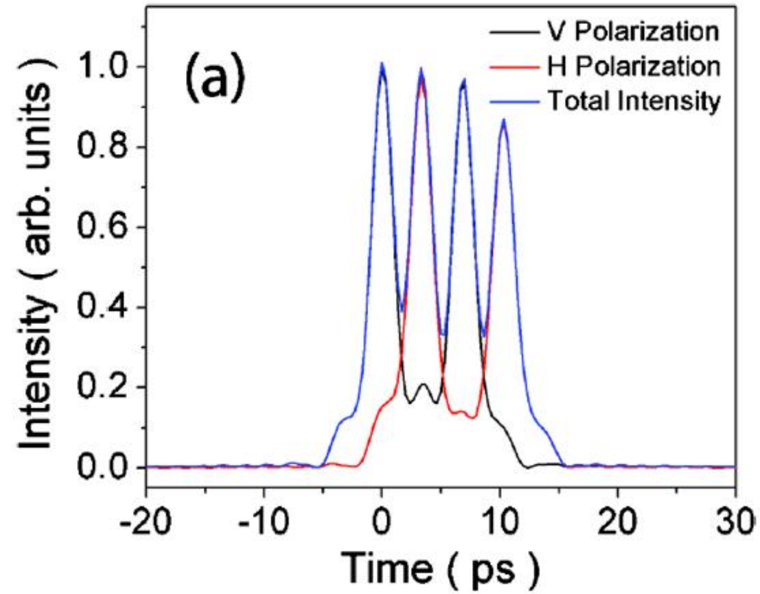

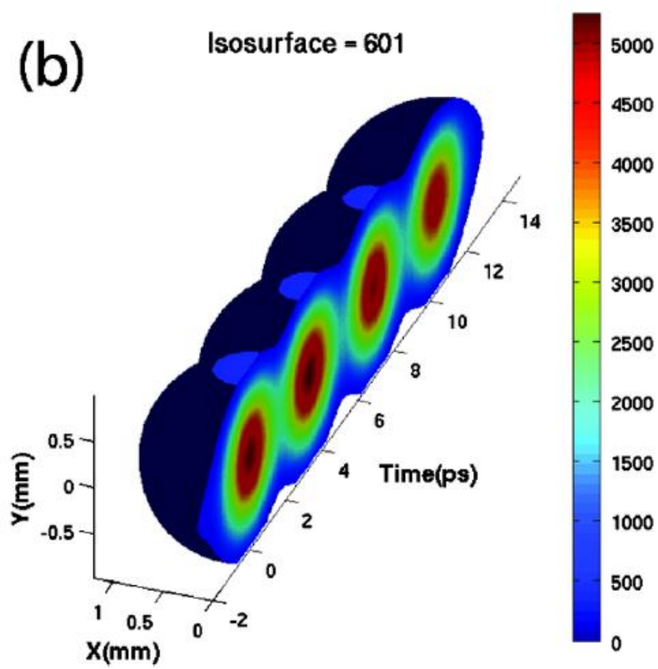

H. Li et al PRSTAB 14, 112802 (2011)

Li and Lewellen 3-d measurement technique

$$I(\boldsymbol{r}) = I_m(\boldsymbol{r}) + I_p(\boldsymbol{r}) + 2\cos\{\omega[\tau + \delta(\boldsymbol{r})]\} \times \int A_m(t, \boldsymbol{r}) A_p[t - \delta(\boldsymbol{r}) - \tau, \boldsymbol{r}] \times \cos\{\phi_m(t) - \phi_p[t - \delta(\boldsymbol{r}) - \tau]\} dt,$$

$$I(\boldsymbol{r}) \approx I_m(\boldsymbol{r}) + I_p(\boldsymbol{r}) + 2\cos\{\omega[\tau + \delta(\boldsymbol{r})]\} \times \sqrt{\Delta t_p i_m(\tau, \boldsymbol{r})} \sqrt{I_p(\boldsymbol{r})}.$$

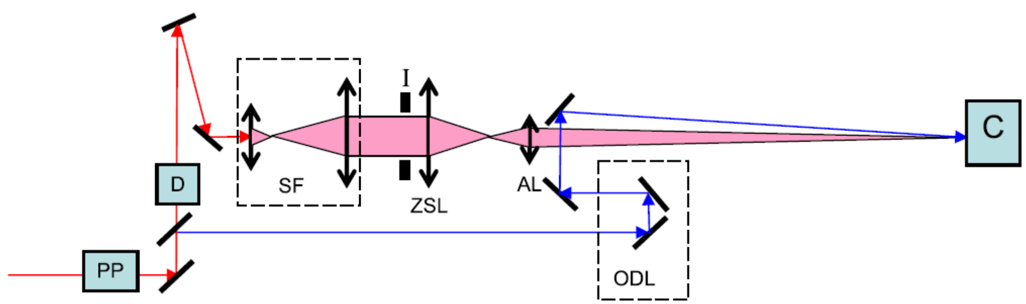

FIG. 7. (Color) Schematic of the experiment. PP: pulse picker; D: DAZZLER; SF: achromatic spatial filter; ZSL: ZnSe lens; AL: achromatic image relay lens; ODL: optical delay line; C: camera. I: iris.

Li et al PRST AB 12, 020702 (2009)

Quasi-ellipsoid proof of principle

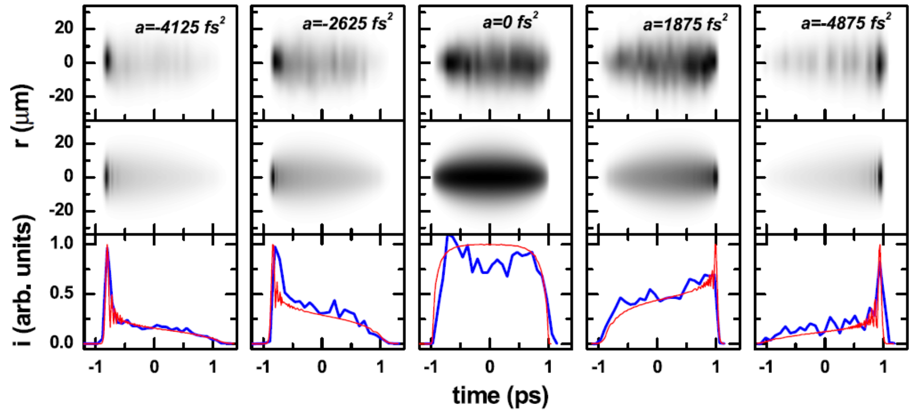

FIG. 10. (Color) Measured (top row), simulated (middle row) spatiotemporal distributions with different linear chirp in the main beam, and the intensity as a function of time at $r = 0$ (bottom row; measured: bold lines; simulated: thin lines). Striations in the experiment data are due to the fluctuation of the laser pointing.

- 800 nm
- phase modulation limited by Dazzler length

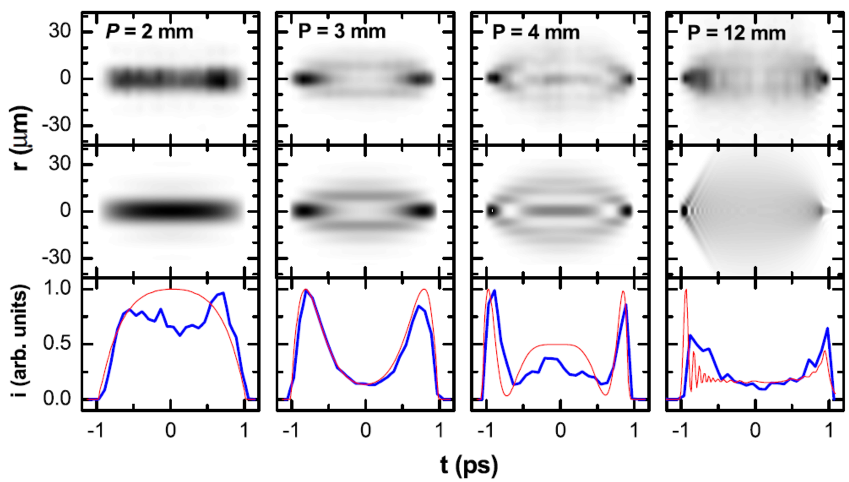

FIG. 11. (Color) Measured (top row) and simulated (middle row) spatiotemporal intensity distribution with different iris radius P using the experiment condition. The bottom row shows a comparison of the intensity at $r = 0$ extracted from the top and middle rows (measured: bold lines; simulated: thin lines).

Li et al PRST AB 12, 020702 (2009)

Pancake pulse

- Self evolving beams (Pan cake scheme)
  - Expansion driven by space charge force

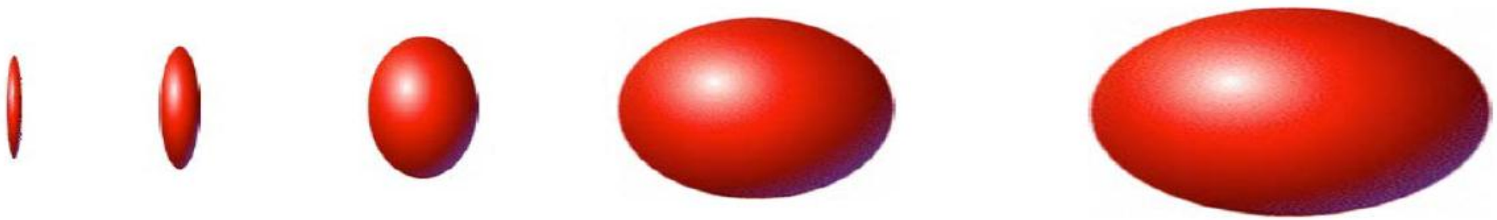

Waterbag recipe:

• Start with a ***flat ellipsoid*** _ can be 'cut out' with 2 intersecting laser beams;
• ***pancake*** _ ***'half-sphere'*** laser intensity profile;
• ***cigar*** _ ***parabolic*** laser intensity profile;
• **automatic evolution into 3D, uniform ellipsoid.**

Erice 2005

L. Serafini, AIP Conf. Proce. 413, 321 (1997)

O. J. Luiten et al., Phys. Rev. Lett. 93, 094802 (2004).

Pancake demo with Pegasus gun

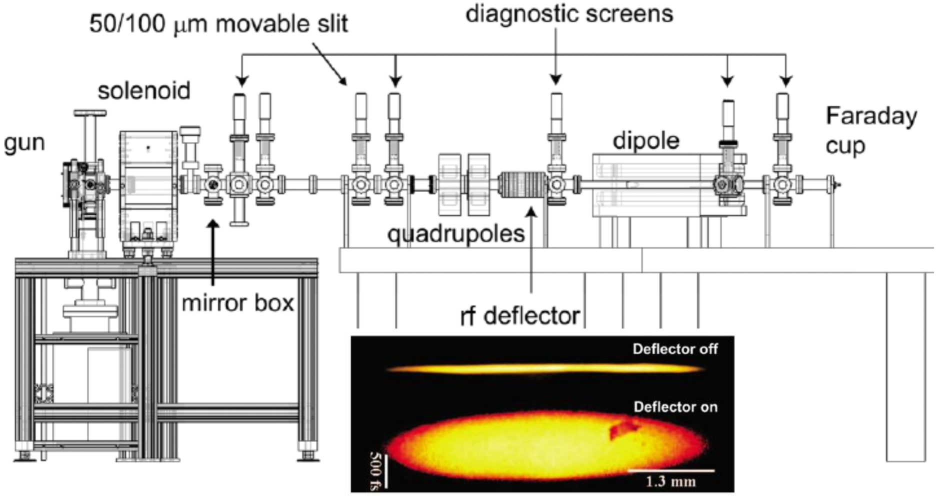

Beam energy	3.75 MeV
Peak field at the cathode	80 MV/m
Injection phase	25°
Beam charge	15 pC
Laser spot size (rms)	400 μm
Laser pulse length (rms)	35 fs

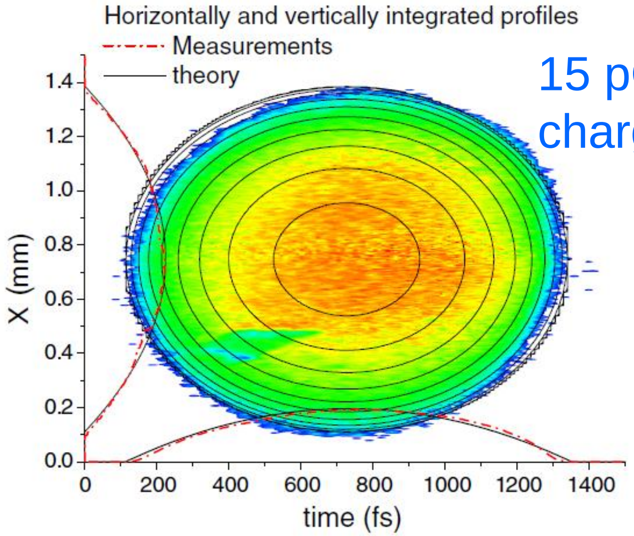

15 pC bunch charge

- Tripled Ti:Sapph laser, Mg Cathode
- Truncated Gaussian, iris radius $r = 0.8\sigma_g$
  - 'half-sphere' shape not required
  - but longer tails, $r > 1.5\sigma_g$ become asymmetric

e^- dist overlaid on ideal ellipse contours, red curves are projections onto axes, black curves are ideal ellipse projection

Musumeci et al PRL 100, 244801 (2008)

Pancake demo with Pegasus gun cont.

50 pC

measured

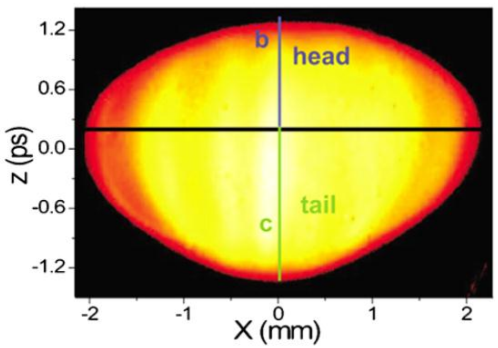

simulated

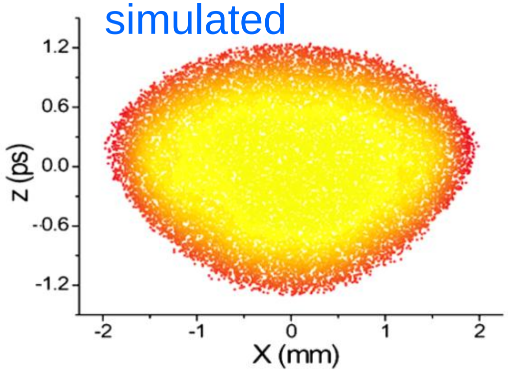

- growing asymmetry with higher charge
- emittance grows with asymmetry
- next step: investigate ability to compensate emittance

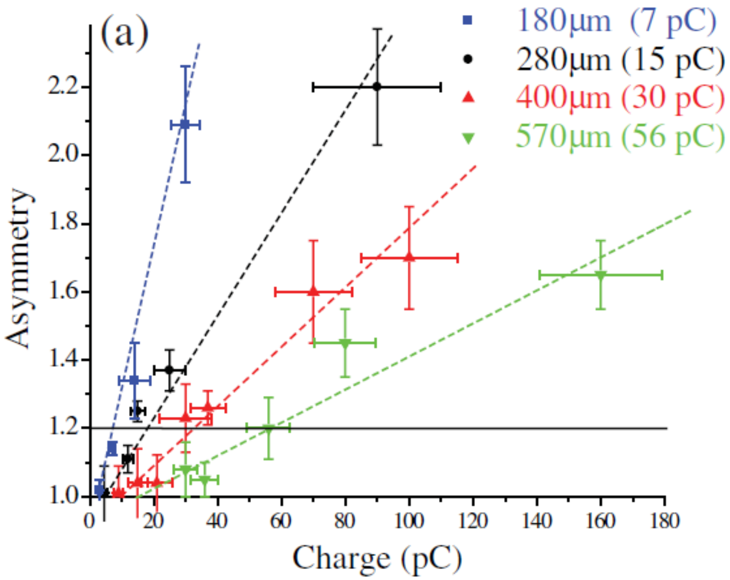

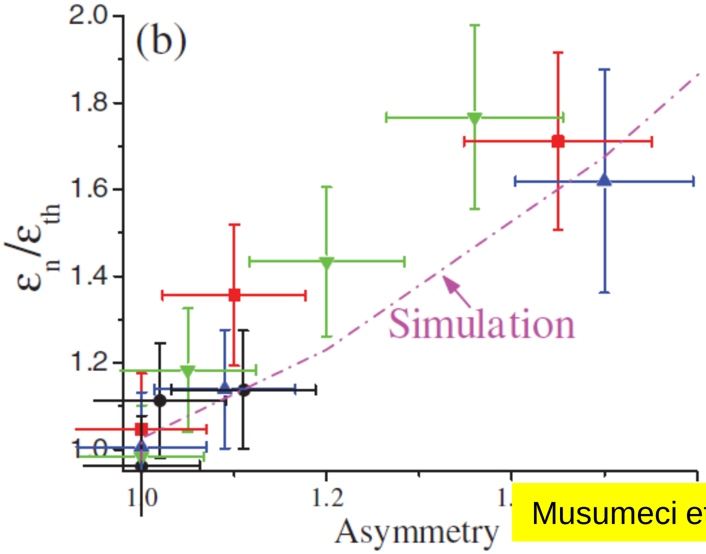

Musumeci et al PRL 100, 244801 (2008)

Z-polarized laser on the cathode & field emission with Schotkky effect (It’s not proved yet!)

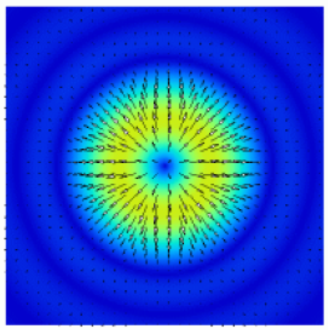

At the focus point, laser electrical field is reinforced in its propagating direction

Radial polarization :

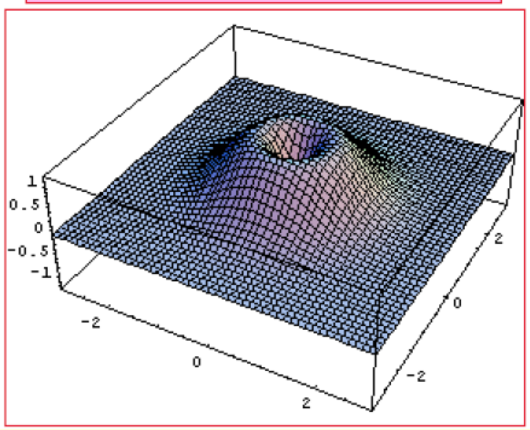

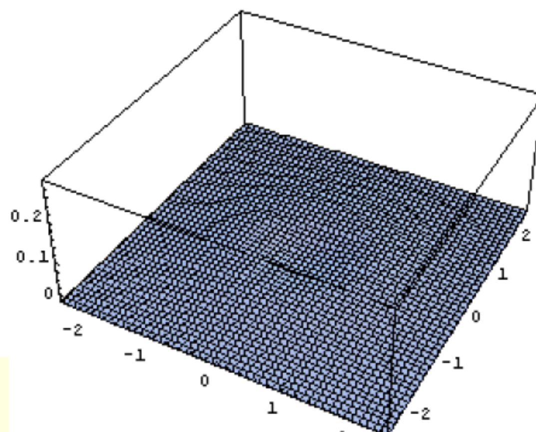

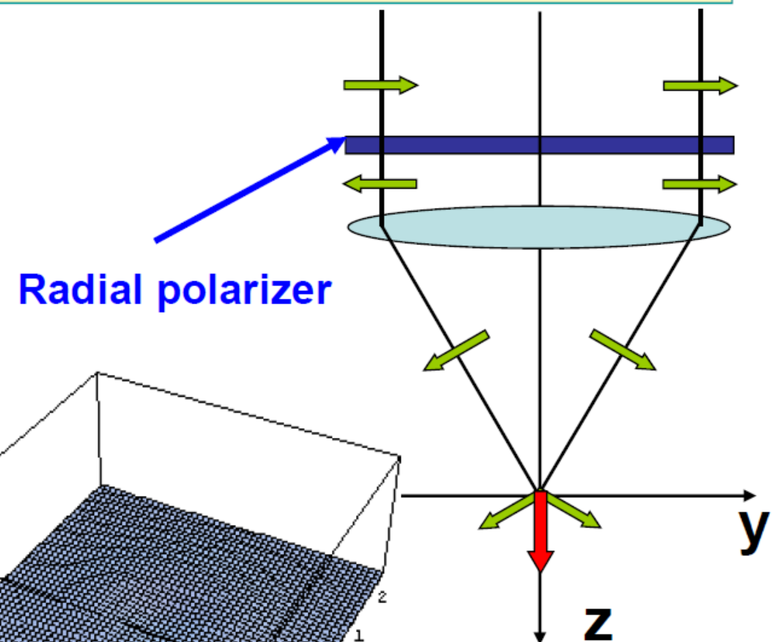

With 1GV/m field,
Work function reduces ~2eV.

H Tomizawa ICFA 2009

Z-field on the cathode surface reduces work function

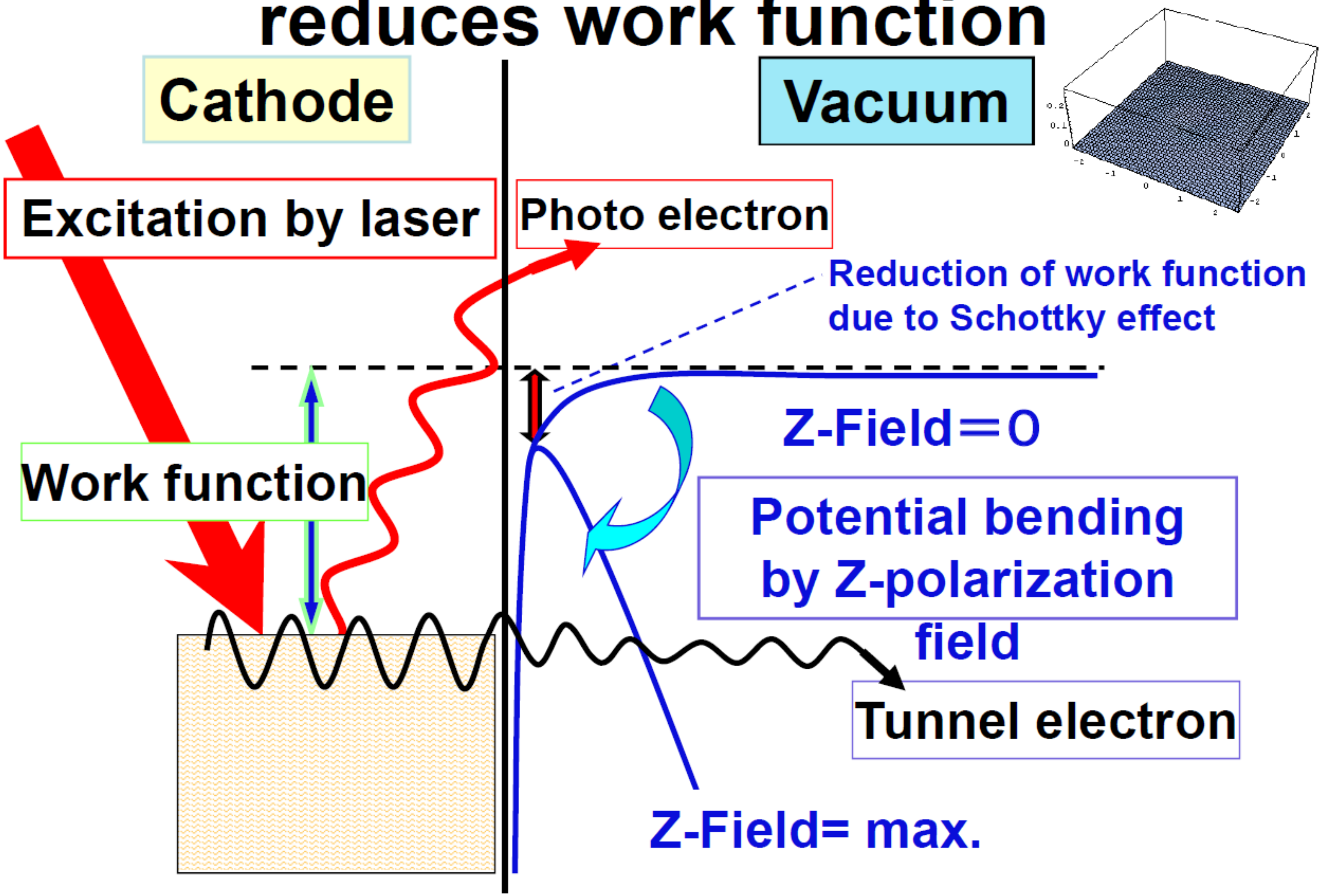

H Tomizawa ICFA 2009

Work function of various metal cathode

With 1~2GV/m field, Work function reduces ~2eV.

Drive Laser wave-length can be IR.

Radial polarization

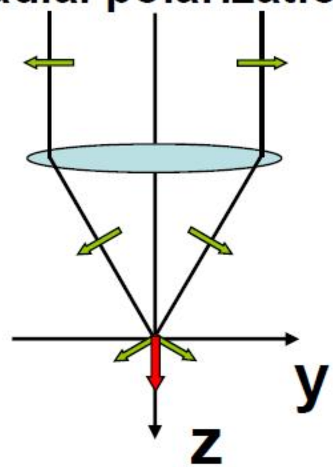

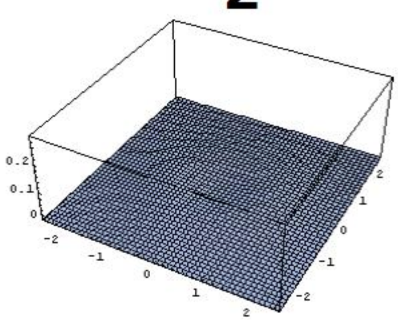

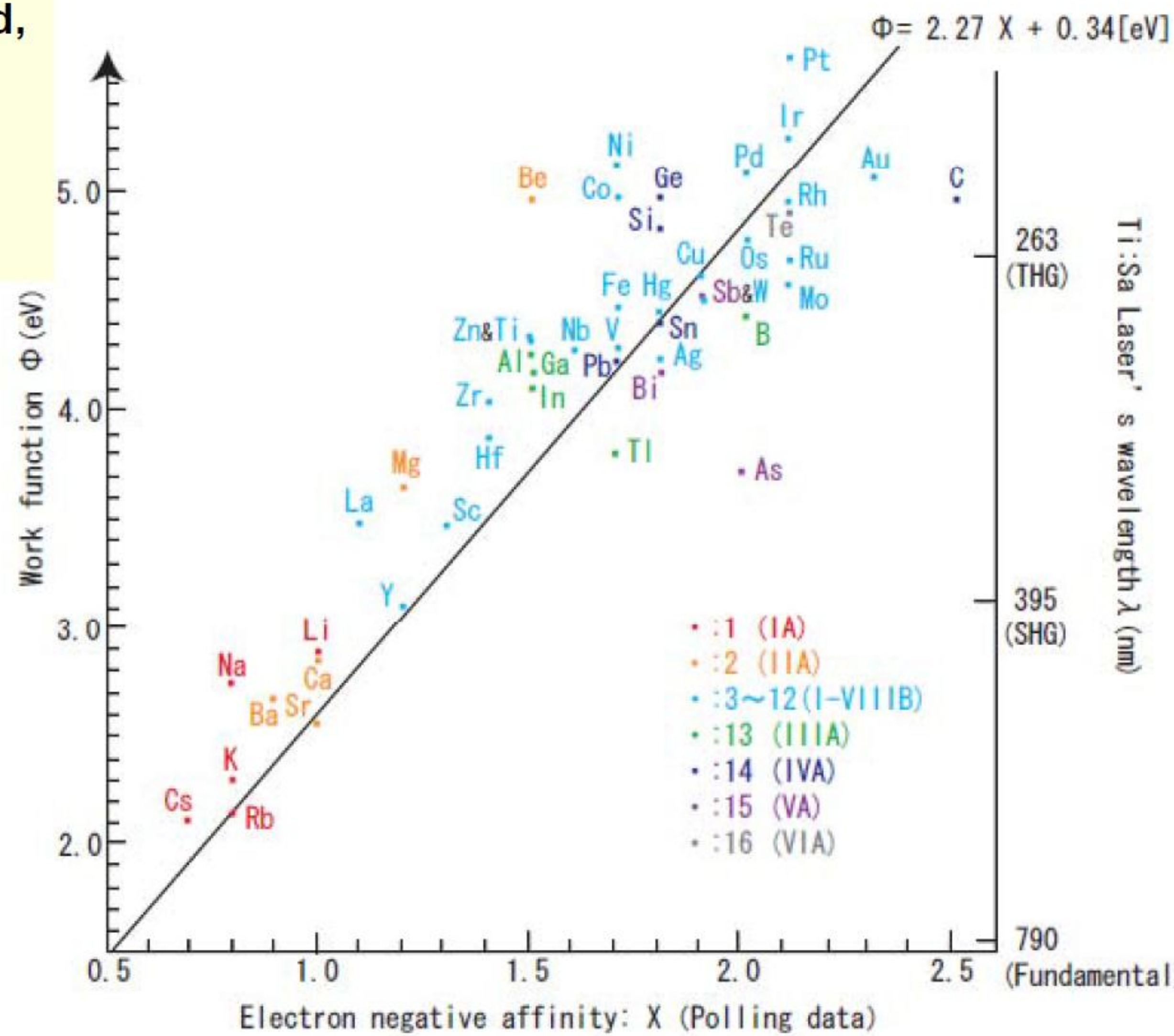

H Tomizawa ICFA 2009

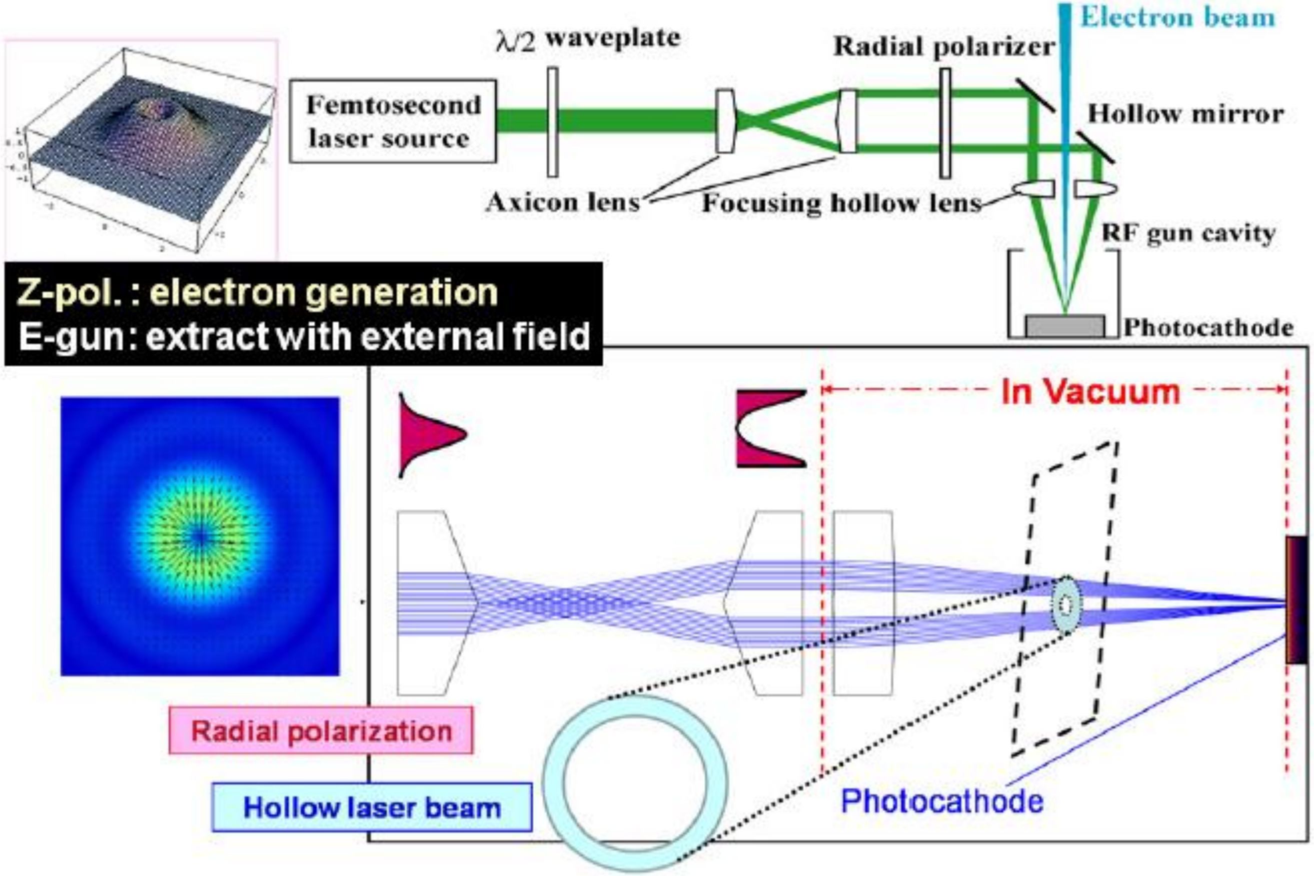

First tests with Copper cathode inconclusive

H Tomizawa ICFA 2010